Addis Ababa University

Addis Ababa Institute of Technology

School of Mechanical and Industrial Engineering

Design, Manufacturing and Experimental Investigation of Pico-Power Hydrokinetic Turbine

---

BY

Teklemariam Tadesse

September 2021

Addis Ababa, Ethiopia

Addis Ababa University

Addis Ababa Institute of Technology

School of Mechanical and Industrial Engineering

Design, Manufacturing and Experimental Investigation of Pico-Power Hydrokinetic Turbine

A Thesis Submitted to School of Mechanical and Industrial Engineering,

Addis Ababa Institute of Technology, Addis Ababa University in Partial

Fulfillment of the Requirements for the Degree of Master of Science in Mechanical Engineering (Thermal Engineering)

BY

Teklemariam Tadesse

Advisor: Dr. Abdulkadir Aman

September 2021

Addis Ababa, Ethiopia

Addis Ababa University

Addis Ababa Institute of Technology

School of Mechanical and Industrial Engineering

Design, Manufacturing and Experimental Investigation of Pico-Power Hydrokinetic Turbine

BY

Teklemariam Tadesse

Approved by Board of Examiners:

1.Dr. Abdulkadir Aman	____________________	________________
Advisor	Signature	Date
2. Dr. Wondwossen Bogale	____________________	________________
Internal examiner	Signature	Date
3. Dr. Muaz Bedru	____________________	________________
External examiner	Signature	Date
4. Dr. Abdulkadir Aman	____________________	________________
Thermal Engineering chair	Signature	Date
5. Dr. Yilma Tadesse	____________________	________________
Dean of SMIE, AAiT	Signature	Date
6. Dr. Ermias Tesfaye	____________________	________________
Director of post graduate program	Signature	Date

Declaration

I hereby declare that this thesis represents my work which has been done after registration for the degree of Masters at Addis Ababa University and has not been previously done in a thesis submitted to this or any other institution for a degree, other qualifications.

Declared by:

Name: Teklemariam Tadesse

Signature: ______________________

Date: ______________________

Confirmed by:

Name Dr. Abdulkadir Aman

Signature: _________________

Date: ____________________

Acknowledgment

First and foremost, I am extremely grateful to my **GOD** and, I would like to thank my esteemed advisor, Dr. **Abdulkadir Aman**, for his invaluable supervision, support, and tutelage during my MSc. Degree and for his treasured support which was influential in shaping my experiment methods and critiquing my results.

My gratitude extends to the school of mechanical and industrial engineering for allowing undertake my studies at the Department of Mechanical and Industrial engineering particularly Thermal engineering, University of Addis Ababa. Additionally, I also thank my friends, workshop workers and, colleagues for a cherished time spent together in the lab, and social settings. My appreciation also goes out to my family and friends for their encouragement and support all through my studies.

Abstract

Ethiopia has plenty of rivers and groundwater sources in the countryside which have the potential to generate electricity from Pico up to Mega power. There is a hydrokinetic turbine technology to generate green energy using river flow water. The gap is to interact with this technology and energy resource of water. The cost of imported equipment for this technology is expensive as well as the available equipment is mostly for large-scale hydropower energy conversion technology projects. This study aims to design, manufacture locally available material and experimental investigation of Pico power hydrokinetic turbine to grasp energy from the river water resource. The hydrokinetic turbine is the systems class of "zero-head" hydropower whereby energy is extracted from the kinetic energy of flowing water, similar to wind turbines, rather than the potential energy of falling water. The method to do this research includes optimizing the geometry of the turbine blade and force analysis of the blade using Ansys software. The blade was manufactured with a 3D printer and the mechanical components were manufactured in the workshop of the school of mechanical and industrial engineering. The test was conducted in four setups at different water velocities. The results are AC RMS value of 11.33Amp and RMS value of voltage 6.89volt respectively with the motor revolution of 486.75 rpm. The power coming from the experiment showed that it is sensitive to current and they have the same sinusoidal pattern plotting the results within each interval of seconds. The net power can be obtained from the turbine was 128.37 watts. The efficiency of the turbine is 51.48%.

Keywords: Hydrokinetic turbine, wind turbine, zero head, hydropower, energy conversion

Acronyms

DC	Direct current
GTP	Grow transformation plan
PLA	poly lactic acid
NAMA	Nationally Appropriate Mitigation Action
CFD	Computational fluid dynamics
CL	Lift coefficient
CD	Drag coefficient
NACA	National Advisory committee for Aeronautics
U	Relative velocity
V_{cav}	Cavitation velocity
TSR	Tip speed ratio
V_{av}	Average velocity
S	Distance of river to measure
U	Rated current velocity
t_{av}	Average time
Cp	power coefficient
ω	Angular speed
F_L	Lift force
F_D	Drag force

T	Torque
C_T	Torque coefficient
C_{ld}	Lift coefficient at design point
M	Pitching moment
CAD	Computer aided design
DC	Direct current
R	Radius of blade element
C	Chord length of airfoil

Symbol

B	Number of blades
D	Diameter of turbine
a	Axial flow induction factor
b	circumference flow induction factor
F	Prandtl tip loss coefficient
f	Tip correction parameter

Greek Letter

λ	Tip speed ratio
ρ	Density
α	Angle of attack
β	Twist angle
ϕ	Fluid inlet angle

η	Overall efficiency
λ_r	Elemental tip speed ratio
k−ε	Computational turbulence model

Super script and sub script

D	Drag
L	Lift
$_{cav}$	Cavitation

Content’s **page**

List of figures **Page**

List of Table **Page**

Chapter 1: Introduction

1.1 Background

The current energy regime in Ethiopia, one that is heavily reliant on the burning of biomass, has had major implications for the environment. The use of traditional fuels as the main source of energy by rural households, which comprise the wide majority of Ethiopia's population, is especially an area of interest. Deforestation, land degradation, decreases in agricultural productivity, and increased greenhouse gas emissions have caused these patterns of unsustainable fuel consumption, and are further exacerbated by Ethiopia's growing population's increased energy demands.

Environmental Policy Review key issue in Ethiopia 2011, by Matthew Cheever etal[1]. reports that the current energy context in Ethiopia, and evaluates the potential for various alternative energy technologies to increase electrification access in rural areas.

The report was carried out through a literature review of institutions governing the energy sector and renewable energy resources and technologies, a spatial analysis exploring energy disparities between rural and urban areas of Ethiopia. Although Ethiopia is reliant on traditional biomass fuels to satisfy its energy demands, there are abundant and diverse renewable resources and electricity generating technologies available that present Ethiopia with the opportunity to move away from the current energy regime[1]. Those renewable energy resources are geothermal, hydropower, wind, and solar energies. Particularly this study is concerned with hydropower energy as well.

Hydropower is suited to areas with steep rivers that flow year-round, a condition which Ethiopia satisfies. Currently, hydropower is the main source of electric power in Ethiopia, with only about 2.4% of the exploitable potential being used [1]. Most of this hydropower generation though is in the form of large-scale operations that delivered electricity through the interconnected System. While hydropower is technically renewable, there are risks associated with near-complete reliance on this form of production, including vulnerability to climate change and geohazards[1].

Due to the precipitation and siltation of the reservoirs, some of the hydropower plants are losing storage volume, resulting in reduced energy output throughout the year. Another restriction of the hydro system is caused by the variability of rainfall [1].

Standing from the hydropower resource Ethiopia can have the potential of generating from Pico to a megawatt of electricity for rural and urban electrification [1]. As we have seen from the Environmental policy of Ethiopia report to build a mega project and some other small-scale hydropower economically difficult to address the electricity service for the rural part of the country pico-power generation is needed for individuals or villages. To generate pico-power the suitable technology hydrokinetic turbine is selected because it has no complex components and is easy to manufacture.

Hydrokinetic was originally developed to surmount the numberless problems associated with dams throughout the world. This system is erected into the river or stream which results in the following advantages compared to conventional hydropower due to its working mechanism being with zero head and not required dam construction. The terms hydrokinetic encapsulate both tidal and river applications. Within the interest of this paper, the focus is on river application, since it is suitable for energy generation in remote and grid isolated areas. The hydrokinetic power generator is operating mostly with zero head only using kinetic principles so it does not need civil work for dam and diverting the direction of water flow implies does not cause reduction of flora and fauna in the rivers[2].

Environmental impacts associated with small-scale hydropower are much less than those connected to larger operations. Small-scale hydro is also amenable to the mini-grid system, making it ideal for rural areas. Like large-scale hydropower facilities though, small-scale hydro is susceptible to periods of drought and the effects of climate change. Reliance on hydropower with little diversification could overcome problems for Ethiopia in the future[1].

Hydropower converts the energy in water flows to useful forms such as electricity or mechanical work. The scales of hydropower capacity range and are generally classified by power output.

Table 1-1 Power output range the given classification [3]

Classification	***Power output***
Small	1-15MW
Mini	< 1MW
Micro	< 100KW
Pico	< 5kw

Pico-hydro is considered as a viable option to electrify remote areas of the country aspect of economic, environmental, and social perspectives. For the off-grid energy alternatives, pico-hydropower has the lowest generating cost compared to a photovoltaic system in 2012 by Bryan Patrick Ho-Yan [3].

Hydrokinetic turbine power production depends on the interaction between the rotor and water. Therefore, an optimum geometry of the rotor must be designed and constructed to capture the maximum water energy and convert it into usable energy. Hydrokinetic energy refers to the energy generated from the moving water of the currents in oceans, tidal, rivers, and artificial water channels. Several technologies have been developed to extract this energy, such as a horizontal axis hydrokinetic turbine and vertical axis hydrokinetic turbine, and other types. Similar to the wind turbine it operates the same principle and it needs to conduct a similar design concept.

The design step starts with the turbine rotor sizing. It is often preferable to have an effective rotor but not too large one as a cost increase with a rotor size[4]. As we know rural electrification is very law so the significant renewable technology is a pico-power hydrokinetic turbine for ruler electrification. However, this technology does not apply to the area of interest up to date in a sufficient manner. A similar study was conducted last year by undergraduate students but it has no good performance in different aspects. So, the design will carry out on the site which gets appropriate data of river flow.

1.2 Statement of problems

The extraction of renewable energy is setting global attention in recent years. To generate energy for the solution of an energy crisis and climate change, we will study alternative renewable energy potential. In Ethiopia, there is hydropower potential energy of 45,000 MW but the big problem was the conversion of this hydropower energy to cover the whole area of the country. Also, rural electrification of Ethiopia with renewables is 8%[5]. This indicates almost there is a small amount of electricity distribution in the rural area of Ethiopia.

The country has plenty of river water sources that have the potential to generate electricity from Pico up to mega power[6]. But there is the technology and resources gap to use the water resource to generate green energy. The cost of imported equipment for this technology is also expensive as well as the available equipment is mostly for large-scale hydropower energy conversion technology projects.

Nevertheless, for a small-scale turbine hydropower technology, it has no suitable cost and sufficient suppliers for small-scale power production of hydrokinetic turbines. Because Manufacturers generally design for flow velocities far over those encountered in real rivers so that actual performance is far below rated output. So, the actual power output is generally limited to a few hundred watts which can charge a battery, power a few LED lights and for light bulbs, etc.

Small-scale hydropower, and in particular hydrokinetic energy systems having high potential in not only off-grid rural areas where as also for small-town electricity sources. But also, in developed countries where a large-scale potential has been extracted and large civil works such as dam construction are not feasible to address electricity coverage over the country.

Now a day there are many researches on this hydrokinetic turbine on performance analysis and experiment. But, there is a lack of interaction between researchers who may have theoretical knowledge while not in real condition. The potential users may have the necessary hands-on practical skills but lack theoretical knowledge to develop this turbine with locally available materials.

So, this study was done on the design, manufacturing, and experimental investigation of the hydrokinetic turbine. Therefore, a locally manufactured hydrokinetic turbine can highly contribute the cost reduction and access to electricity for rural areas as well as can satisfy the future hydrokinetic turbine technology.

1.3 Objectives of the Research

1.3.1 The general objective of the research

To design, manufacture, and experimental investigation of Pico-power hydrokinetic turbines.

1.3.2 Specific Objective

- Modeling and sizing of the blade
- Sizing the main components of the turbine
- Hydrodynamic performance analysis of the blade
- Manufacturing of the turbine
- Conducting experimental test setup

1.4 Significance of the study

According to S. Tsegaye's report about the Ethiopian energy sector, the electric demand will be expected to grow by 32% for consecutive four years until 2025 [7]. Pico-power hydrokinetic turbine proved rural electrification for the off-grid area near to the coastal population and some other villages nearest to the river or individual families. Its implication develops off-grid rural electrification which is set by the energy sector of Ethiopia. Mainly having the role for the advancement of this hydrokinetic turbine for rural electrification and it will give benefit for a local manufacturer of hydrokinetic turbines.

1.5 Scope of the study

The scope of this thesis carries out an analysis of hydrodynamic performance and its sizing of mechanical components, simulation for the forces exerted on the blade in operation and the pressure distribution and streamline velocity of the blade but not the entire system, and manufacturing of pico-power hydrokinetic turbine and experiment set up.

1.6 Expected outcome the study

The expected outcome of this thesis is to design and manufacture and experimental investigation of the pico-power hydrokinetic turbine to generate the desired electricity as per the design specification and try to get the power output with the range of 150-250 Watts and address rural electrification easily.

1.7 Limitation of the study

In this study, the experimental result only measures current and voltage due to the unavailability of measuring instruments. The torque and power are getting calculated from the experimental result of current-voltage. The manufacturing accuracy of mechanical components which are shaft, bearing and, pully, and belts is not enough based on the design.

1.8 Organization of the study

The organization of this study has five chapters and the detailed organization of each chapter is presented here.

Chapter one discussed the background of the study and concept of a hydrokinetic turbine as well as power classification. Chapter two discussed the household energy demand of Ethiopia, its socio-economic advantage, and the previous study on the performance of the turbine blade. The criteria to remove the cavitation are based on the amount of lift to drag coefficient ratio.

Chapter three has four different categories which are discussed in the introduction on the main operational feature of hydrokinetic turbines and the parameters that affect blade performance. the basic theory of blade design. The second part discussed the overall design of the turbine which are the blade and its mechanical components. The next categories discussed the manufacturing of the blade and other components of the entire assembly of the hydrokinetic turbine. The last discussed the experimental setup and electrical circuit properties.

Chapter four discussed the results and discussion of the result got from the experiment. Finally, chapter five was discussed on conclusion and recommendations.

Chapter 2: Literature Review

2.1 Introduction

Ethiopian government undertakes, growth and transformation plan (GTP) in the transition from developing country to middle-income country by 2025. To achieve this goal sector of agriculture and industry is significantly considered. Therefore, the power sector is expected to grow simultaneously to fulfill the energy demand of the population. An endowment of Ethiopia's renewable energy resources has the potential to generate beyond 60,000 megawatts.

To increase energy generation capacity, around 10,000 megawatts from hydropower per year and must increase energy generation beyond this amount of power for the future energy demand. This hydropower covers 86% of Ethiopia relative to other renewable energy of the country but still for rural electrification coverage is very small which is 8% [5].

Hydropower is the free emission energy compared to most of the other energy sources. The energy-generating system is suitable than the other source of energy to keep environmentally friendly due to almost being free of emission of greenhouse gases [2].

The technology of small-scale hydropower is still in going of development and the functionalities are not yet fully explored. Small-scale hydropower has a growing interest around the world, and different concepts have been tried out with various results. As mentioned, the company Tropton Energy Service has twenty years of experience in the field of hydrokinetic turbines and has worked in the UK, Sudan, Somalia, Egypt, and Peru. They claim to have success in implementing their technology in remote areas and have done a case study where a farmer in Sudan got irrigation water for his 12 acres of land relying on their Garman turbine” [8].

Hydrokinetic power is a function of water density (ρ), flow velocity (v), swept area (A)of the turbine, and zero head hydrokinetic turbine is a river current device that takes water kinetic energy to generate electricity without changing the water level. Design and construction of a small hydro turbine electric generator that can be made based on the economic user potential to afford it, and to develop the power generation with this system need to consider free environmental pollution and quality of power to the user in the rural area.

The construction and mass production of this mini hydrokinetic power plant will serve as an alternative to power generation for domestic and small industrial consumption there by pulling such load off the national grid, which will then help the transmission company to redirect their power to heavy load center in the country, thereby improving power quality, power security and reliability of power to the end-users [11].

2.2 Rural electrification of Ethiopia

Most developing countries are facing the problem of energy depletion locally available energy resources and are dependent on imported fuel. The core problem next to the food shortage energy crisis needs to care with a high degree. This situation happens in Ethiopia and traditional fuel contributes to 99.9% of rural parts of the country. The biomass energy for household consumption is 97% is very high compared to some other African countries such as Burundi, Kenya, Somalia, Sudan, and Uganda, and rural electricity sources 5% in 2014[8].

Ethiopia is often described as the water tower of northeastern Africa. It was estimated that the country has a hydropower potential of 40,000 MW installable potential. Not more than 3807 MW has been utilized so in percent it is about 90.5 % of the potential unused [9].

The average electric potential energy is excellent, while the wide range is covered by hydropower. A small-scale plant without the use of a reservoir is approximated to about 20 TWh/year and has a great significance for rural electrification [10]. Ethiopian population living in rural areas in scattered turf. Providing a grid is not economical for the area of interest, to tackle this problem off-grid rural electrification with the help of renewable energy, alternatively, small-scale hydropower technology is highly guaranteed for they are living in the riverside [11].

The household lighting of Ethiopia as per the report of the world health organization clean fuel and technologies are used for lighting purposes with electricity, battery-powered, lantern, and solar energy. Almost 30% of the household, however, uses harmful(pollutant) fuel and technologies for lighting purposes, including kerosene and wood[12]. The overall lighting consumption of fuel and technologies in Ethiopia is shown below.

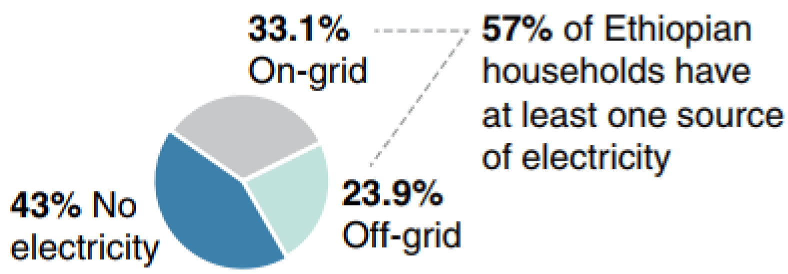

Figure 2-1Grid and off-grid access of Ethiopia in 2019 [13]

In Ethiopia, access to electricity for lighting purposes in the urban area is large, however in rural areas too small electrification. To expand the electrification of the countryside the country has a plan to use hydropower potential so as the pico-power hydrokinetic turbine is significant[12].

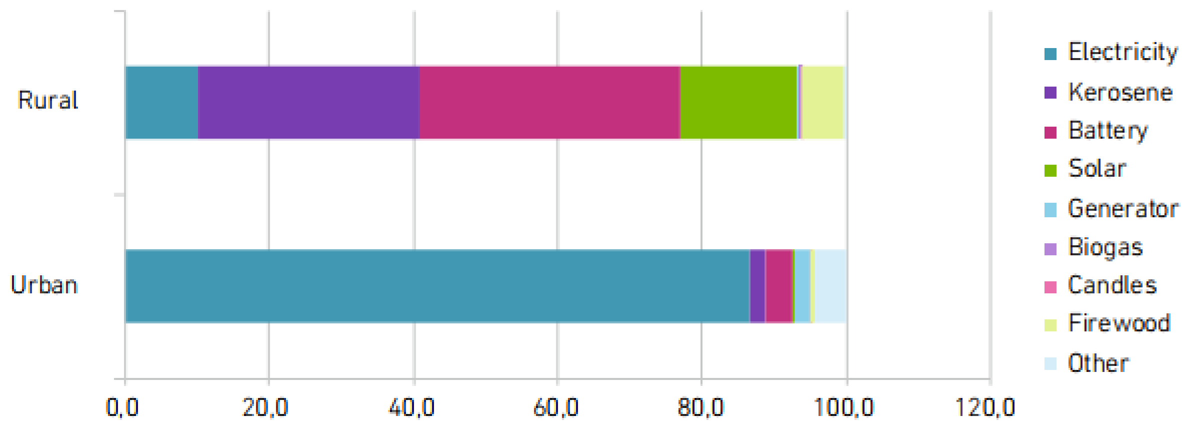

Figure 2-2Lighting fuel and technologies used in urban and rural parts of Ethiopia, 2015 [14]

The proposed **Nationally Appropriate Mitigation Action** (NAMA) will help accelerate off-grid energy access is mainly faster and cost-effective rural electrification with clean and modern energy sources. As proposed by NAMA is "The off-grid rural electrification NAMA is a step towards overcoming the barriers and achieving transformational change in the rural electrification sector"[14]. The electrification gap between rural and urban areas of the country is too large as we see from the figure below.

Time Period		Total Households	Off-Grid Connections Added	Cumulative Off-Grid Connections	Off-Grid Access Rate
Program	Year	(millions)	(millions)	(millions)	(percent)
GTP II	2017	19.9	0.0	2.2	11%
	2018	20.4	0.0	2.2	11%
	2019	20.7	0.1	2.3	11%
	2020	21.1	0.5	2.8	13%
	2021	21.6	0.7	3.5	16%
GTP III	2022	22.0	0.9	4.4	20%
	2023	22.4	1.0	5.4	24%
	2024	22.8	1.2	6.6	29%
	2025	23.2	1.5	8.1	35%

Figure 2-3 Grid connections program and universal electricity access (2019–2025) [13]

To reduce this gap of electricity access between those areas of the country need to design and manufacturing of pico-power hydrokinetic turbine is significant. And it can provide electrification and can handle expensive consumption of fuel, reduce greenhouse emissions, and keep flora and fauna due to no need for civil work for the dam or diverting direction.

2.3 Socio-Economical Benefit of Hydro Power

Most Ethiopian population use biomass energy for day-to-day activities moreover in rural areas of the country. When we introduce hydrokinetic turbine technology for the sack of using the potential of renewable energy. It is also an environmentally friendly and cost reduction system. In recent years researchers introduce pico-power hydrokinetic turbines for rural electrification. Because it can manage environmental pollution from the emission of burning biomass and low construction cost. “Rural electrification is often financially viable as the willingness to pay has been commonly found to exceed the long-run cost of supply. This implies good rates of return and financial stability. However, this is dependent on two major factors: supply costs and system losses must be minimized, and a balance must be struck between financial stability and reaching the poor [3]. Rural electrification can benefit the environment.

Electricity is a high-quality form of energy that can be used for many applications. It is typically generated more efficiently while emitting little pollutants compared to the burning of traditional energy sources such as liquid fuels or wood biomass for lighting or heating purposes. There is a greater dependence on wood fuel in poorer countries than in richer countries. There is an increasing trend in electricity consumption per capita as country wealth increases [3]. The electric coverage is good and can use low-cost generation of power based on their income implies that it can mitigate energy crisis within magnitude as well as protect climate change.

As we know the operating principles are kinetic principles with zero head. As a result, it needs to study efficient turbine selection and structural optimization of the rotor which is to get expected output power. The selection of optimal hydrokinetic turbines is significantly considered [18].

There are two types of selections the first method is that selecting a turbine based on head and flow rate these are called humble rules. The second method is the Scientific method:

Given the complexity of designing a new hydro turbine for a particular location and application, initial turbine technology selection should be based on not only technical, but also social, environmental, and economic factors conventionally; turbines have been mainly selected based on the specific speed [19].

The main aim of this study is the manufacturing of improved efficiency pico-power hydrokinetic turbine as explained above the design scheme of this turbine is analogous to a wind turbine, the design starts from the rotor blade and size. Because the amount of power generated depends on the relation between the water channel and rotor blades.

2.4 A related previous study on the Performance of Rotor Blade

There are different types of rotor blades based on their performance. Monatrakul [15] effect of blade angle on turbine efficiency for a spiral horizontal axis hydro turbine. Modeling and a computational fluid dynamic (CFD) analysis were conducted to examine the maximum rotational force of the turbine. The turbine blade angle was varied to 15, 18, 21, and 30 degrees at water velocities of 1, 1.5, and 2 m/s respectively. Findings from the calculations were compared with a conventional 3-bladed axial turbine under conditions with and without a collection chamber.

The study reveals that turbine efficiency with a collection chamber is higher than that of free-flow, and the blade angle has a significant effect on turbine efficiency[15]. Another investigation was conducted by Hamzah et.al. [16] on the effect of blade number on performance Savonious water turbine in the water pipe. The experiment shows that the 3-blade generator turbines had a higher amount of power if compared to the 2- blade, 4-blade, 5-blade, and 6-blade turbines. The 3-blade turbines generated power of 2.992 Watt, 6.304 Watt, 19.122 Watt, and 34.834 Watt on each debit variation even though 3 bladed turbines have balance and can resistance of vibration[16].

For micro-hydro turbines, the extraction of energy evaluated the multi-stage and single-stage with the velocity range of 0.5m/s to 1m/s comparatively multi-stage is good performance than a single-stage blade. Based on this result the author recommends testing this multi-stage blade turbine by increasing velocity range and to model energy generation more than five stage blade[17]. In a similar concept, many researchers have evaluated different types of hydrokinetic turbine blades based on the angle of attack for the horizontal axis, vertical axis, and spiral hydrokinetic turbine and they have given their result justification.

The fluid flow analysis could be applied to determine the hydro foil shape producing and the optimum lift and drag force. In the case of wind turbine development, the selection of foil could be able to improve the energy efficiency from the various MARIN-designed turbines. There are several steps to vary the foil shape that is by changing the chord and chamber. The first step is by changing the chamber width only. The proper selection of chamber will give a contribution to the enhancement of lift force but the drag force will increase as the chamber widened. The effect of fluid-structure interaction is analyzed to obtain the influence of the lift and drag force changes [18].

The second step is by changing the chord length and chamber width together. Lift and drag coefficients are obtained based on the variation of both components. On the other hand, the angle of attack is also varied to produce the same magnitude of lift force although the length and width of the foil are different. In addition, lift and drag force are considered, there is one more phenomenon that should be avoided is the stall. This phenomenon causes that the stability of foil is unstable because the ratio between drag and lift coefficient is the most of its value. The critical angle of attack is the angle of attack which produces the maximum lift coefficient. This is also called the "stall angle of attack". Below the critical angle of attack, as the angle of attack increases, the coefficient of lift (Cl) increases. Conversely, above the critical angle of attack, as the angle of attack increases, the air begins to flow less smoothly over the upper surface of the airfoil and begins to separate from the upper surface [18].

For the conversion of energy using a hydrokinetic turbine, the blade profiles having a small angle of attack are usually selected where CL and CD are increased and decreased respectively. The design of hydrokinetic blade profile which the ratio of CL and CD was chosen for the study and to select the profile considering the large section and thickness to overcome the mechanical force produced during operation of the blade and avoiding increasing of drag. The optimization of blade profile for the sake of conversion of the kinetic energy of water flow with zero head to electricity with the satisfaction of cost [19].

Yining [20] conducted a study on the influence of the chamber on hydrodynamic characteristics of the airfoil. In the numerical simulation of airfoils with different camber, the effect of camber on airfoil's performance was only considered, while other factors were not taken into consideration. Airfoil's performance is affected by the overall geometry, such as camber, relative thickness, the position of maximum relative thickness, and position of maximum camber. However, camber has a greater influence on it. Therefore, to improve the hydrodynamic performance of airfoil, other influencing factors and cavitation should be considered comprehensively.

To maximize the hydrokinetic turbine power output and assure good enough strength, the blade structure hydrofoil must be designed carefully [21]. Ismail et.al [22] was investigated the comparative study on the river considers the possible blade profile of a hydrokinetic turbine for adequate utilization of energy production. The turbine must be easily manufactured blades and easy to install, replace and maintain. Four blade profiles were investigated, that is, flat plate, circular arc, NACA 0018, and NACA 1548. CFD simulations showed that circular arc profiles are more efficient and produce more power[22].

The performance of hydrokinetic turbine currently has a maximum of $C_p=0.35$ found on most tests with the water velocity of ranges of 0.8 m/s-1m/s [23]. On this system, the performance tried to increase the performance beyond 0.35 and reduce the manufacturing cost of the turbine.

2.4.1 Turbine blade number and its TSR relation

The turbine with two-bladed can produce energy at TSR of more than 11 but with those TSR and number of the blade, more than three is impossible to produce torque. Implies a low number of blades operate at high rotational speed resulting from moderate angle of attack and it produce moderate lift force and high bladed turbine operates at low speed due to low angle of attack the lift also low. For the generation of electric power, the turbine must operate at high rotational speed and this leads to a medium number of a bladed turbine with medium TSR considering geometric optimization of the turbine blade. The method to determine the coefficient of performance of the blade versus to tip speed ratio blade element model is better than CFD, wu. et al [24].

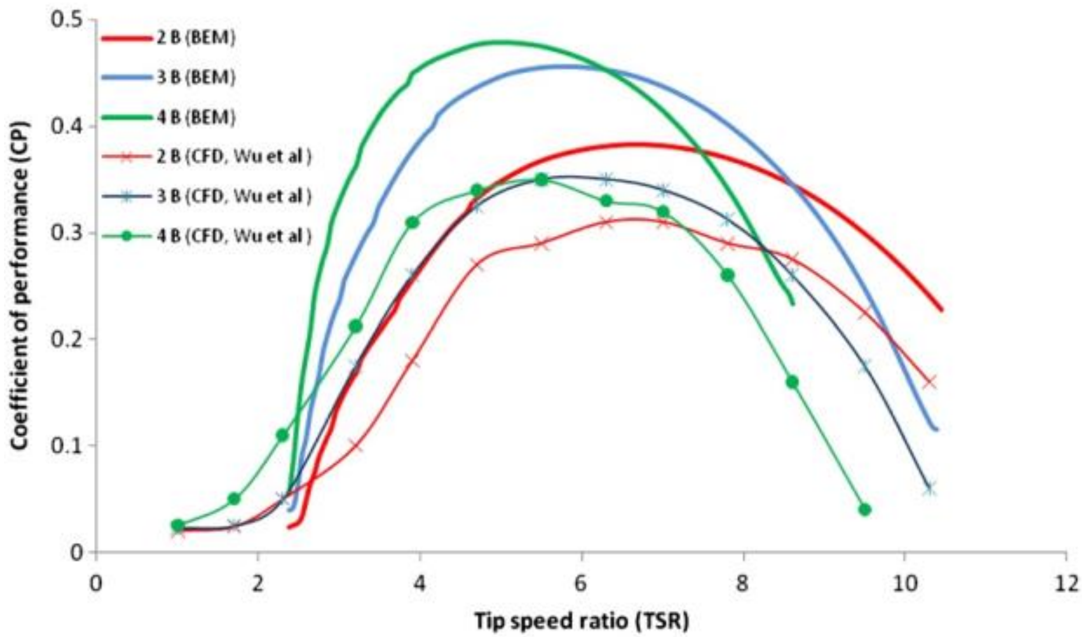

Figure 2-4Coefficient of performance vs to TSR variation of blade number [22]

Hydrokinetic turbines bring newer advantages and greater possibilities for better hydroelectric power generation. For this reason, achieving a very high lift blade rotor to take the maximum kinetic energy advantage for rivers with a slow velocity flow is very important. A very low inertia rotor permits a self-starting effect for the axial water flow turbine to take the maximum advantage of the river kinetic energy which is very important in this kind of device.

2.4.2 Cavitation removing criteria

Cavitation is the phenomenon that should be considered in the design of a hydrokinetic turbine blade. The effects of this phenomenon cause structural damage to the blades, reduce their performance, and generally originated in the blade section where the pressure decrease below the vapor pressure of the fluid. The fluid vaporizes instantly forming a cavity of vapor which changes the flow.

The size and the shape of the bubble vary as a consequence of the action of the pressure and the velocity field. When the cavity is intransitive the pressure on the surface of the blade increases and develops erosion on the blade. This effect causes a decrease in the lift and an increase in the drag leads to a reduction of the turbine efficiency [25]. The efficiency and performance of the rotor are mostly dependent on the shape of the hydrofoil used. Generally, thin hydrofoils deliver more efficiency than thick ones. However, from the structural strength point of view, the thickness of the cross-sections of the hydrofoils near the blade root should be increased. The design thickness of the blade sections depends also on the span length and the hydrodynamic requirements. In large rotor diameter turbines, relatively thicker hydrofoils should be employed to accomplish structurally strong.

The main goal of blade and wing design is to increase the lift coefficient and decrease the drag and pitching moment coefficients. Cavitation is the biggest restriction in choosing a hydrofoil for a hydrokinetic turbine rotor. Thin blade sections especially the hydrofoils that are used at the blade tip are more susceptible to cavitation. To design a high-performance rotor, the cavitation number should be as low as possible while the lift coefficient and the lift to drag (Cl/Cd) ratio should be as high as possible [26]. Aerodynamics and Hydrodynamics disciplines are similar, but the study of hydrodynamic requires taking care of ventilation and cavitation phenomenon. Turbine working in riverbed operation avoids the possibility of being affected by ventilation events. Cavitation is produced on the outer surface due to the low pressure of the incompressible fluid produced in its neighborhood; it depends on water temperature, airfoil profile, and flow velocity. As higher the velocity is, the higher the cavitation possibility [27].

To optimize hydrodynamic design considering cavitation simplified model to avoid cavitation in each blade section is employed together with the classical Glaurt's optimization. The criteria to avoid cavitation requires that the relative velocity U at each blade section along the radial coordinate must be smaller than that of cavitation velocity (V_{cav}). i.e., relative velocity U is greater than the cavitation velocity the local relative velocity must be corrected. Using the blade element momentum theory method the blade element for the calculation of the chord length replacing U by V_{cav} in the section where $u \geq V_{cav}$ leads to an increase in the chord changing the pressure condition on the blade [28].

2.5 Material for turbine blade

A turbine rotor hydrofoil made in the composite material can be designed for this purpose. The material design aspect of the blade for this hydrokinetic turbine composite material is as good as that of the classic or one type of material structure [29]. The hydrokinetic turbine experienced hydrodynamic loading. So, the strength and toughness are considered as fussy selection material properties from the operation point of view. Another criteria corrosion resistance and weldability are both important attributes to be considered when selecting an alloy for a turbine blade from the maintenance point of view.

The final material properties chosen for the turbine blade are density and its strength. A low density is a better roll for good running performance as well as increased efficiency of the system as the lighter blade will rotate more easily[30].

This hydrokinetic turbine has not been as efficient and accessible as required by studies so far. Therefore, the purpose of this study is to achieve the desired goal and meet the needs of the user.

A dual nozzle crossflow turbine performance would have a better performance compared with the conventional crossflow turbine. It is because the water jet power hitting the turbine blade is more evenly and well guided. The water energy obtained from the nozzle is effective and pushes more turbine blades compared with the horizontal single nozzle cross-flow turbine or the vertical single nozzle crossflow turbine. The most optimal efficiency was generated by the crossflow turbine with a dual nozzle, which is 78.80%, while the crossflow turbine with a single horizontal nozzle efficiency reached an efficiency of 70.78.%. For the crossflow turbine with a single vertical nozzle, efficiency reached the lowest efficiency of 61.92 %. But the cost-effectiveness is expensive than that of single crossflow turbines [31].

The above-mentioned literature has an investigation of their findings to increase the performance of the hydrokinetic turbine studying with different parameters. The result of the finding was good, but the problem is when implementing this technology not yet get the design power output over to the actual power generating from the turbine.

This study overcomes this deviation by identifying parameters to increase performance and manufacturing with locally available materials for the future technology of this zero head hydrokinetic turbine.

Chapter 3: Materials and Methods

3.1 Introduction

The general principle for obtaining energy from flowing water is the hydrostatics of the hydrodynamic method. The hydrostatic method uses the water in an artificial reservoir to form a constant flow of pressure and the potential energy from the water head hits the turbine blades for energy conversion. The hydrodynamic method has no artificial dams or reservoirs and is only used as a continuous flow of water with zero kinetic energy running through it. Place hydraulic turbines in the river to convert them into electricity [32].

The principle is similar to that of a wind turbine. Its energy conversion capacity depends on the speed and density of the water, the area swept by the blades, and the efficiency of the turbine. Its theoretical maximum value is 0.593, which is called the Betz limit. Only high-efficiency turbines operating with low mechanical losses under optimal conditions come close to this limit. Although the efficiency of small river turbines is usually below this limit.[32].

The basic theory of blade design: Moment theory refers to the analysis of the control volume analysis of force in the blade based on the conservation of linear momentum and angular momentum, while the blade element theory refers to the analysis of the force in the blade section as a function of the blade geometry [33].

Blade Element Moment Theory (BEM) is a model used to evaluate the performance of a rotating turbine based on mechanical and geometric parameters and the characteristics of the interacting flow. This model is the result of the combination of two theories: the theory of the element of the blade and the theory of the moment.

The first was introduced by William Froude in 1878 to study the behavior of turbines from a local perspective. In this framework, the turbine blade is cut into several parts, and each of the elements of the blade is approximated by a flat model. This method leads to an expression of the force exerted on the blade element as a function of the flow characteristics and the geometry of the blade. The basic quantities of the model are two experimental coefficients (usually represented by CL and CD), called lift and drag coefficients, respectively, which account for the force in the cross-section as a function of the angle of attack, that is, the relative angle between interaction blade and flow of water. Then integrate the result across the sheet to get the global value [34].

The blade element momentum theory continues to be mainly applied to wind turbines, as initial aerodynamic analysis, conceptual design, load, and stability analysis, and control design, as well as fluid power turbines.

The parameter that affects the performance of hydrokinetic turbines is their mechanical generator Efficiency and the interaction between fluid and blade geometry. This study focused on blade geometry, such as rotor diameter, water flow rate, blade tip speed, chord length, angle of attack, and blade fit. The detailed analysis of these parameters will be discussed in the design section below.

3.2 Methodology

The method or procedures to achieve the objectives of the study follows in such away;

Review the previous related works that are reviewed to examine and understand clearly the stated problems.

The data collection system are primary and secondary data. For the primary data are river flow data from minister of water, irrigation and energy, actual measuring of Jemma river velocity using floating method. Secondary data collects from different related article, books, video journals etc.

Modeling and sizing of a hydrokinetic turbine blade, the hydrodynamic performance analysis of the turbine, and sizing of mechanical components of the hydrokinetic turbine as well as geometric optimization of the blade have been done to meet desired performance. The hydrodynamic performance analysis will be carried out with the computational method by changing different parameters to investigate the blade performance.

The next step was be studied locally available material properties suitable for the optimized blade of the turbine with different criteria to meet the desired performance of the blade. At the end of this task, manufacturing the blade and experimental testing of the pico-power hydrokinetic turbine was be conducted at the design site of the river.

The designed and manufactured components are blade, hub, frame (motor stand) and the components to be selected are motors, shaft, pulley, and belt.

Flow chart diagram of the method

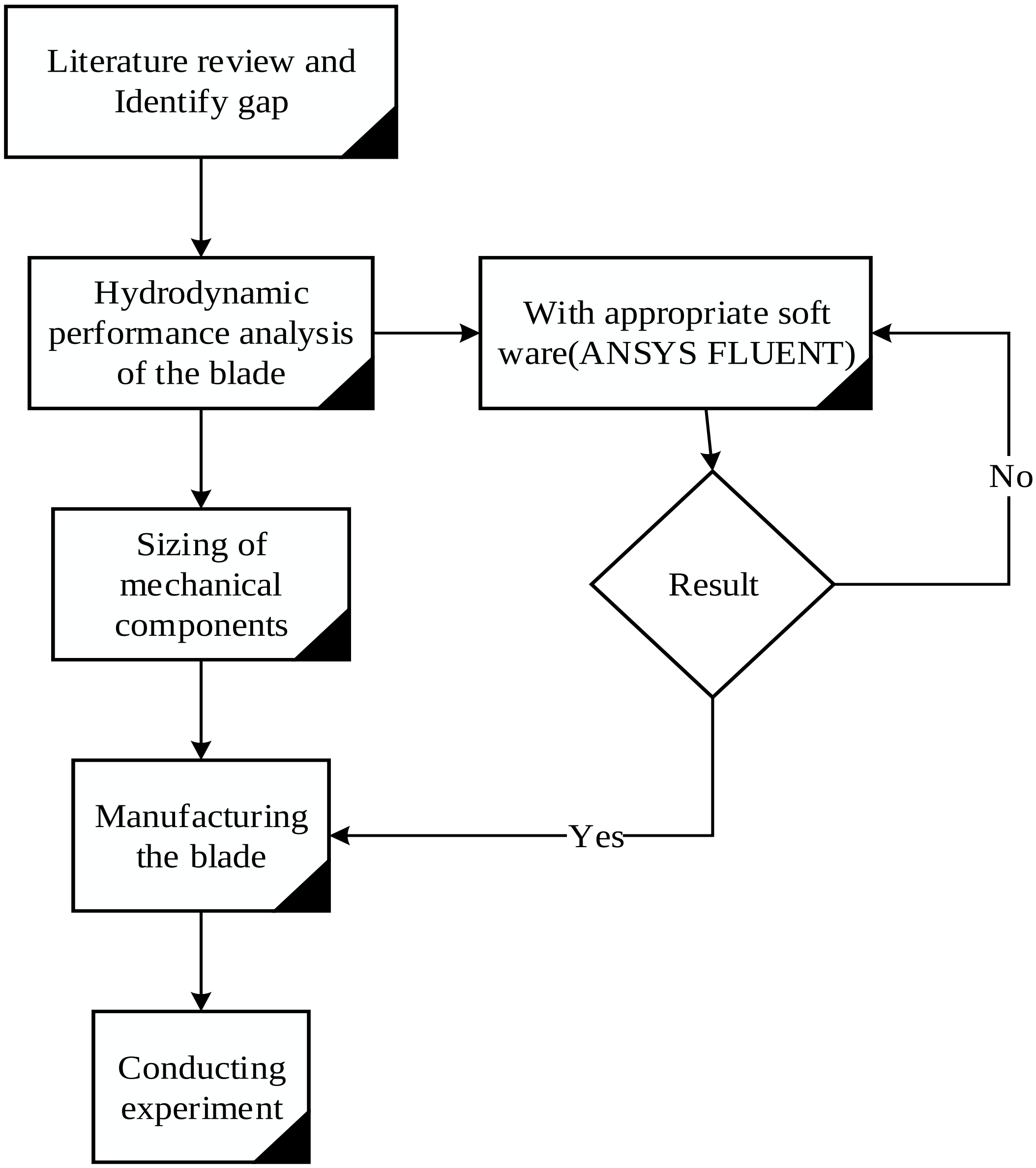

Figure 3-1 Flow chart diagram of the methodology

3.2.1 Components of Pico –Power Hydrokinetic Turbine

The components are classified based on their mechanical and electrical works which are;

- ✓ Hydrokinetic turbine blade,
- ✓ Hub,
- ✓ Cotton belt

- ✓ Transmission shaft,
- ✓ DC Motor
- ✓ Stand or frame.

3.3 Conceptual layout of the proposed design and its working principles

3.3.1 Conceptual layout

The conceptual design represents the simple layout of the system and it is possible to understand easily the working principle of the turbine.

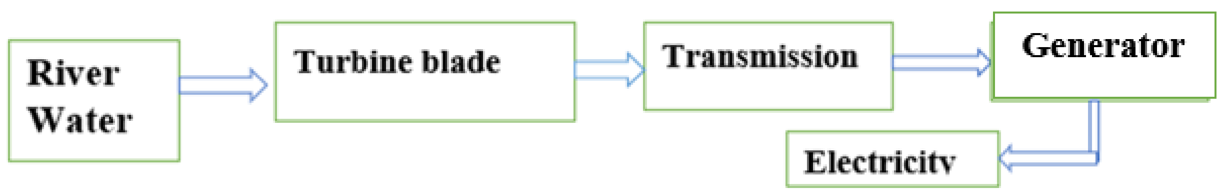

Figure 3-2 Conceptual layout of a pico-power hydrokinetic turbine

The pico-power hydrokinetic turbine is under a flowing river or in a low-speed channel with zero head because of turbulence. The turbine rotor starts to rotate due to the kinetic energy of the water and produces mechanical energy. This mechanical energy develops torque on the generator shaft to turn the shaft and then converted into electrical energy by a DC motor, thereby generating electrical energy.

3.4 Design of Hydrokinetic Turbine

Understanding the blade theory applicable to hydrodynamic turbine blades is critical because the performance of a hydrodynamic turbine depends on the number of blades allocated to the rotor and the design parameters of the blade elements. Blade theory states that the outer contour of the blade must comply with aerodynamic considerations, and the materials used in its manufacture must be able to provide the necessary strength and structural rigidity. This means that during the design and development of the propeller or rotor blades, extensive inspections of aerodynamic factors and the properties of the materials of manufacture are required.[35].

As mentioned in the literature the hydrokinetic turbine is analogous to the wind turbine in the design aspect because this hydrokinetic turbine is operated within zero head. The working fluid used for the hydrokinetic turbine is water and for a wind turbine is air so the mechanism to produce electrical energy is similar means that the design procedure is also similar. The only difference in the fluid properties which are its viscosity and density of water and air, a test and verification of the characteristics of an airfoil in the water are required [36]. The water density is approximately 890 times greater than air, which is leading to greater forces and greater power density and it needs a waterproofing device [37].

3.5 Material selection of the blade

As we know all engineering and commercial materials have many properties such as physical, mechanical, chemical, electrical, magnetic properties and production ability, product shape, material cost, the impact of material on the environment, availability, aesthetic and recycling, etc that have been studied and accepted in material science and engineering literature.

The optimum material that fulfills the specific requirements are engineering and commercial material experts apply the knowledge in engineering. Production engineering, as well as material science and engineering, include expertise in selection, design, analysis, fabrication, and evaluation of specific engineering or commercial material in their various forms and different operating conditions to develop target property for an application [30].

As mentioned in the literature of selection criteria of materials for the target applications are material reliability 36%, production volume 23%, cost factor 17%, availability factor 13%, maintainability 8% get from the customer point of view. This magnitude indicates the most important criterion to selecting material for the hydrokinetic turbine is reliability [38]. Reliability is an important factor to be during the design of a hydrokinetic turbine blade. The overall hydrokinetic turbine system depends on the critical role of turbine blade reliability developed by time-dependent analysis [39].

3.6 Suitable types of hydrokinetic turbine

Commonly there are two types of hydrokinetic turbines similar to wind turbines based on the axis of rotation. Which is the horizontal axis and the vertical axis turbine and in addition to a hydrokinetic turbine there is also oscillating -foil hydrokinetic turbines and have their features. Based on features of exiting hydrokinetic turbine a horizontal axis type is selected for this study. This hydrokinetic turbine is can be fixed to the riverbed or seabed, to an anchored floating platform, or can stick on a rigid body out of the water.

Models that are fixed to the riverbed or seabed are the most common; although access is harder, they are more unobtrusive visually. Currently, they are the main hydrokinetic turbines in development around the world [40]. Regarding the efficiency of the horizontal axis turbine, the maximum value of C_P is 0.59. the value reported for the axial wind turbine is as high as 0.5 but the vertical axis is 0.31 maximum value measured for the Gorlov turbine [41]. For this reason, the horizontal axis turbine is selected.

3.7 Site selection

The main important thing to design and installation of this hydrokinetic turbine is a suitable site selection. The site for this design of the turbine is Jemma river downstream across Ankober in front of Alem Ketema for the reason it is very far from the main grid, the community sets near to the riverside and the community lives on the area are moderately dense[42]. The flowing river permanently flows over the year but in summer and winter the flow may not be equal and to consider, fluctuation of flows, the turbine is designed as an easily movable turbine on the surface of the water to regulate the power generation. The transportation of Jemma is not difficult to transport the turbine components, even though the components are not too large they can easily ship off to the turbine installation yard.

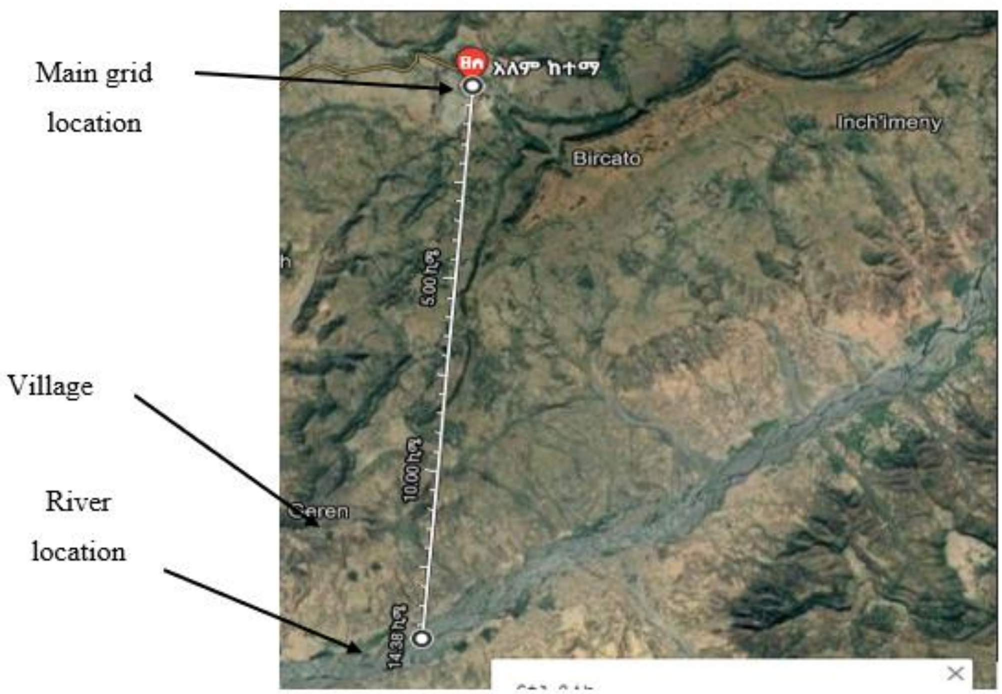

Figure 3-3 Representing of the distance between the main grid and river

Chapter 4: Design Analysis

4.1 Determination of turbine design components

To determine the turbine design elements, we need to know the basic design parameters shown below:

According to the types of applications, the tip speed ratio is different. For electric power generation use $4 < \lambda < 10$ and the number of blades selected based on this range from the table below.

Table 4-4-1Suggested blade number, B, for different tip speed ratios [43]

λ	***B***
1	8-24
2	6-12
3	3-6
4	3-4
>4	1-3

The blade number is 3 the λ value >4 otherwise fewer than this it needs considering wise hub design because of structural problems [43]. The current wind turbine has not used an even number of rotor blades, the reason is the stability of the turbine.

The turbine with an odd number of rotor blades which is at least three (3) blades can be considered to be similar to a disc calculating dynamic properties of the machine. Due to this important reason, the major turbine design available in the market has this number of rotor blades. The selection of the number of blades depends on the fluid profile but in general design context and available in the market have three blades turbine rotor [44].

4.1.1 Define the blade shape

To obtain and examine the empirical curves for aerodynamic properties of an airfoil at each section (the airfoil may vary from the root to tip.) i.e. $C_L vs\alpha, C_d vs\alpha$. To choose the design aerodynamic condition $C_{ldesign}$ and α_{design} is maximum that or the ratio of $C_{d,design}$ to $C_{l,design}$ is at a minimum for each section.

The modern HAWT turbine blades have been designed using airfoil, that the design of blade tip is using a thin airfoil, for high lift and drag rotation. The Reynold number found in wind turbines in the interval of 500,000 up to 10 million. Aviation airfoils such as the NACA 44xx and NACA230xx where the popular airfoil was chosen because they have a high maximum lift coefficient, low pitching moment, and low minimum drag.

NACA series classification has 4, 5, and 6 wing sections, for wind turbines 4-digit series is generally used. The design procedure and its operation principle of the hydrokinetic turbine are analogous to a wind turbine as mentioned earlier, as a result of this turbine also used 4 digit NACA series hydrofoil [43]. As explained in the above works of literature the most suitable airfoil for hydrokinetic turbine energy conversion purpose is the **Sxxxx family's** airfoil at constant Reynold number. Generating the data from the NACA series of Sxxxx a comparison was made between four types of Sxxxx families foils.

According to Anyi Martine, et al[45]. investigation Sxxx was adopted for hydrokinetic because of its resistance to fouling or less sensitivity to dirt than the conventional NACA section. Because of the dirty nature of the rivers, the fouling resistance characteristics of the Sxxxx family profile are highly desirable in the hydrokinetic turbine.

From those airfoils taken the NACA series as mentioned above Sxxxx performs well at constant Reynold number and is the most efficient hydrofoil used in hydrokinetic turbine. So selecting the suitable shape from the NACA series are S1020, S1210, S1221, and S2046. The angle of attack taking 5^o and the Reynold number 1000,000, Ncrit number 9 C_L/C_D vs alpha are get maximum. The data was generated online using an airfoil generator.

The Ncrit value is a measure of free-flow turbulence and is used to simulate the transition position when the forced trigger position is not provided. XFOIL adapted from eN transition theory. Used to simulate fluid turbulence or airfoil roughness. The Xfoil documentation has a partial explanation of this method and a table of suggested values (reproduced below).[46].

Table 4-2 Ncrit value for different value [46]

Situation	Ncrit
Sail plane	12 to 14
Motor grinder	11 to 13
Clean wind tunnel	10 to 12
Average wind tunnel	9
Dirty wind tunnel	4 to 8

Here, the two-dimensional panel code XFOIL is used for the aerodynamic design of the wind turbine airfoil. In this code, the eN method can be used to simulate the laminar turbulence transition through the NCRIT parameter, depending on the disturbance level (DL) of the airfoil operation. DL is related to free-flow turbulence, wall roughness, and vibration level.

Table 4-3 various NCACA Sxxxx foil

NACA series	***Ncrit number***	***Reynold number***	***Angle of attack α***	***Max.CL/CD @ α 5***
S1020	9	1,000,000	5	146.8222
S1210	9	1,000,000	5	145.1803
S1221	9	1,000,000	5	126.1849
S2046	9	1,000,000	5	68.63804

For S1020, S1210, S1221, and S2046 the graph was generated respectively.

As we have seen the curve S1020 airfoil performance on the interval of the angle of attack -20 to -10 is constant and a little drop around -7.5^0 angle of attack. But from -5^0 to 12.5^0 indicates a rapid increment of lift to drag coefficient ratio until 5^0 and it is the maximum value and the curve above this maximum value angle attack up to 12.5^0 rapid decrement while beyond this an asymptote with the axis of the angle of attack.

The airfoil performance curve (S1210) is zero in the interval of -10 to -6 and until the angle of attack of 6^0 moderate increasing of C_L/C_D. But above this maximum value slopped decreasing performance. So, the maximum value achieves 0 to 6^0 angle of attack and the peak value at 6^0.

The performance curve of S1221 is a similar pattern to the S1210 curve. The increment and decrement behavior is the same on the specified interval of the angle of attack. But the difference on both curves (S1210 and S1221) is the peak value which is the maximum value for S1210 is at 6^0 angles of attack 147 and for S1221 at the angle of attack 7^0 has 133.82.

This S2046 airfoil performance on the given range of angle of attack has a sinusoidal pattern. As indicated on the curve from -20^o to 0^o a high drop of performance particularly at -11.5^o angle of attack and it returns to zero and increases the performance with a constant slope up to 5^o of the angle of attack. The maximum performance achieves at 8.75^o angles of attack but it is not sufficient relative to other airfoils.

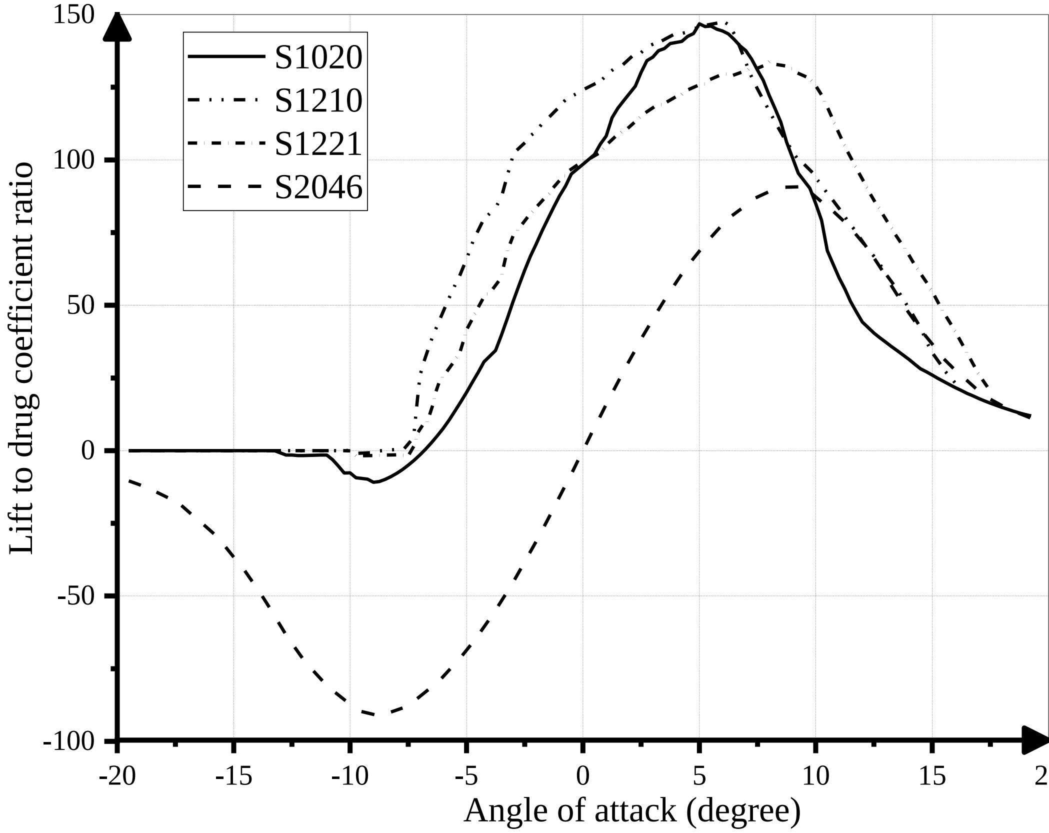

Figure 4-1 Performance curve for selected airfoil

As we have seen all airfoil curves S1020 have better performance relative to the other curves plotted in figure 3.7. For good electricity generation of a hydrokinetic turbine having an angle of attack less than 10o.the particular angle of attack of the NACA series airfoil is minimum around the selected angle of attack of 5°.

The maximum value from the graph of C_L/C_D vs alpha (α) S1020 @ alpha 5 is 146.822.max and the maximum thickness was taken from NACA series 15% of the chord at 33.8% from the leading edge and maximum chamber 4.6% of the chord at 57% from the leading edge. This airfoil is generated using QBlade design software but the values vary slightly on C_L/C_D and its maximum thickness and maximum chamber.

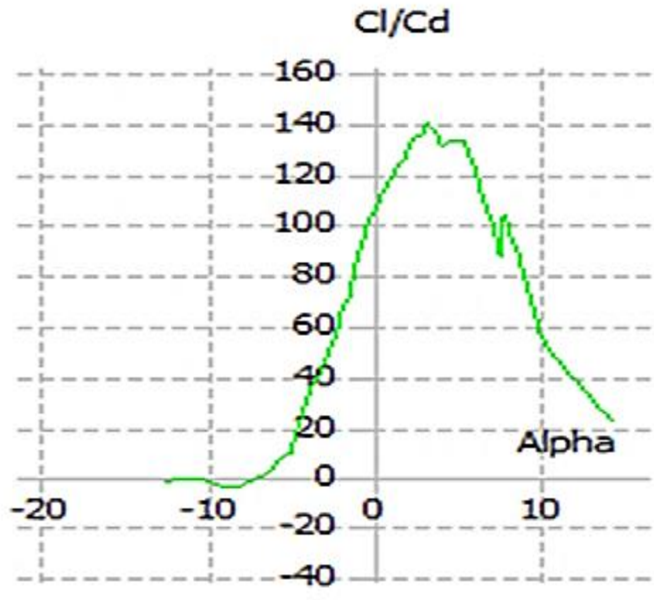

Figure 4-2 performance curve using QBlade design of S1020

The performance curve generated by QBlade design software diminished by 4.5 % from the curve generated from the NACA series for the selected S1020 airfoil. As it indicates the maximum performance gain at an angle of attack 5^{o}. Therefore, the design and model of airfoil this turbine blade at this angle of attack.

Table 4-4 Representation of thickness and camber using QBlade

Thickness	15.09	Coordinate location
Max. thickness	33.90	X= 0.00827301
Maximum camber	5.05	
Max. camber position	52.05	Y= 0.308543
Number of panels	61	

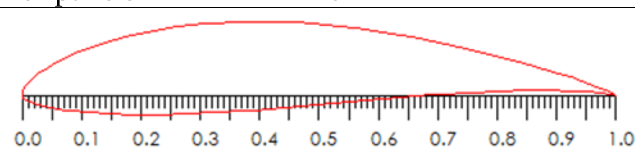

Figure 4-3 airfoil shape generated from QBlade software

Based on the result the turbine blade is designed as follows. The design parameter is provided in table 3.5.

Flow measurement data of the river

The velocity of the river flow is necessary for sizing of the rotor and performance analysis which is the main parameter of the activities required for the study. The swept area of the rotor taking the estimated value of the velocity was determined using the equation (3.2). But the flow data of the river in the specified site is not available and it needs actual velocity measurement.

There are different methods to measure the velocity of the river and the way to measure within each method are have their accuracy, ease to do so, and cost-effectiveness. The easiest method is the floating method and selecting this method because it has no need for more electronic materials, other related measurement instruments, as well as its accuracy, is acceptable. The surface float method measures the time required for a buoyant object to float along the surface of a stream over a given distance. If the object is only partially submerged, and there is no wind, the object's velocity should equal the water velocity at the water surface. For the surface float method, a water fillable plastic fishing (tough bubble) was used as the floating object and a floating fishing line was strung through the float for easy retrieval.

The instrument and procedure to measure using the floating method

1. Tape measure
2. Stop-watch (cell phones often have a timer)
3. Yard or meter stick to measure depth (tape measures are more difficult to use)
4. Three highly visible buoyant objects such as sticks or logs, pine cones, or oranges (objects heavy enough not to be affected by the wind)
5. Stakes or rocks for anchoring tape measure to channel banks (can act as markers)
6. Optional waders (you will usually get wet if doing this correctly)

The flowing river is at least a 10-meter distance(straight) of an inscribed place and it is a smooth flow river and taking the average velocity which is taking an average time because the measurement applies at least three times the velocity is multiplied by correction factor 0.85 for the depth of the river is 1meter[47], [48] Mathematically expressed, $V_{av} = S/t_{av} * 0.85$, where the distance is constant but the time is varying recording at least three times or more than this on the given distance.

The distance taken from the river to the flow direction is 10 m and it has been measured three times based on the method. So, the recording measure of the water flow in the river was performed on both sides of the river and finally took results on the middle of the river. Put two marks on the side of the river at the distance of 10 meters in between two marks. When to start recording time, the light stick drops on the surface of the water until it will reach to the next mark. Then after taking the time to cover the given distance. Therefore, the recoded data are shown below in the table.

Table 4-5 Measured flow data of the selected site of the river

	Region of river	***Time in second***	***Average Time***
1	North	12.5	11.33333 sec.
2	At the central location	10	
3	South	11.5	

To determine the velocity for this study we need to multiply the correction factor (0.85)

$$V_{av} = S/t_{av} * 0.85 \qquad (4\text{-}1)$$

$$V_{av} = \frac{10}{11.33333} * 0.85 = 0.75 m/s$$

Figure 4-4 Measured River for the design interest

The location of the river is found in north Shewa in Merhabete woreda and its flow direction is east to west. The potential of the river at Lemmi station is represented in figure 3.7.

The flow duration curve of the river at Lemmi station represent in table 3.6

Table 4-6 Flow duration of Jemma river at Lemmi station[13]

Year	1983	1984	1985	1986	1987	1988	1989	1990	1991
Q(m^3/s)	83	80	84	65	39	47	71	90	57.6

Year	1992	1993	1994	1995	1996	1997	1998	1999	2000
Q(m^3/s)	65	102	72	59.5	123	78	55	69.5	52.5

Year	2001	2002	2003	2004	2005	2006	2007
Q(m^3/s)	85	84.2	67	86	83	79.5	87

The lowest annual recorded mean annual flow of 2.15 m3/s occurred in 1973 and corresponds with a period of drought. The highest mean annual flow of 7.13 m3/s was recorded in 1977. The Jemma at Lemmi is one of the tributaries of the Abay River and represents the local drainage of the central part of the western Ethiopian highlands. The other rivers in the upper reaches of the Jemma, Muger, and Guder are intermittent and were not flowing during dry periods of the observed years [13].

Table 4-7 design parameters of the turbine

S. No	***Design parameter***	***Values***
1	Estimated power, P [W]	250W
2	Estimated power coefficient, *Cp*	0.45
3	Estimated efficiency coefficient	0.8
4	Rated current velocity, U	0.75 m/s
5	Water density	1000kg/m^3
6	Estimated Tips speed ratio	7
7	Blade number	3
8	Angular speed ω	73.012 rpm

The net power delivered to the end-user is

$$p = 0.5\eta\rho v^3 A \tag{4-2}$$

But at the design point

The estimated power is 250W, efficiency including the losses of the rotor. Bearing and gear, generator efficiency is 0.8 because the mechanical components are compatible with generators typically have an efficiency of about 0.9. A modern generator may have an efficiency of about 0.9

and we take 0.8 based on this efficiency, the density of water is 1000kg/m^3 and the velocity from the river measurement is 0.75 m/s the area to size the blade is determined below.

$$A = \frac{2\times p}{\rho \times 0.8 \times V^3} = \frac{2\times 250}{1000\times 0.8\times 0.75^3} = 1.4815 m^2$$

The diameter is 1.374 m. and its radius R is 0.687m. because the radius of the rotor depends on the power extracted from the turbine. For the energy conversion process, various losses are to be considered.

4.1.2 Rotor design

The rotor is the main energy conversion component of the hydrokinetic turbine and its efficiency is determined directly by the overall efficiency of the turbine. Based on the blade element momentum method HARP_Opt (Horizontal Axis Rotor Performance Optimization) utilizes a multiple-objective genetic algorithm and blade-element momentum theory flow model to design horizontal-axis wind and hydrokinetic turbine rotors [49]. HARP_Opt optimizes a rotor's execution for relentless and uniform streams (no sheared or yawed streams). An assortment of rotor control arrangements can be planned to utilize HARP_Opt, counting settled or variable rotor speed and settled or variable blade pitch moment. Blade with circular or non-circular roots can be outlined utilizing HARP_Opt. HARP_Opt can work as a single- or multiple-objective optimization code. The most optimization objective is to maximize the turbine’s vitality generation. For hydrokinetic turbines, extra imperatives are characterized such that cavitation will not happen. An extra objective can be enacted, in which HARP_Opt performs a structural optimization to play down the edge mass [50].

The efficiency of the blade broadly depends on the shape of the hydrofoil occupied. The objective of the hydrofoil is to highly develop the lift coefficient and to reduce the drag coefficient and pitching moment coefficient. Also, cavitation is an important phenomenon in selecting hydrofoil for hydrodynamic turbine blades.

Designing the hydrokinetic turbine as explained earlier similar to wind turbine need to follow the principles of aerodynamics, structural dynamics, material science, and economics are to be applied to develop a machine that is reliable and efficient [51]. The hydrofoil design can be done in two different methods which are hydrodynamic design and its structural design. The good performance of the external profile of the blade is provided by hydrodynamic design. The principal requirement of hydrofoil design is high C_L and high C_L/C_D over the wind range of the angle of attack to obtain optimized performance[21].

The turbine size is determined by

$$P = \frac{1}{2}\rho A V^3 \tag{4-3}$$

Angular speed

$$\omega = \frac{60\lambda_0 u}{\pi D} = \frac{60\times 7\times 0.75}{3.14\times 1.374} = 73.012 rpm \tag{4-4}$$

chord length

$$C = \frac{8\pi r}{BC_{LD}}(1-\cos\phi) \tag{4-5}$$

Where C_{ld} is the lift coefficient at the design point. From the performance data of the airfoil, the values of angle of attack and lift coefficient are taken and used in the design. This angle of attack identified at which drag to lift coefficient ratio is minimum. The design procedure involves computing chord length C and blade setting angle β at a different section of the airfoil. The mathematical expression of those parameters of the blade section at distance from the center of the rotor.

$$\lambda_r = \frac{\lambda_D r}{R} \tag{4-6}$$

The fluid inlet angle ϕ,

$$\phi = \frac{2}{3}\tan^{-1}\frac{1}{\lambda_r} \tag{4-7}$$

Under the constrained condition

$$b(1+b)\lambda_r^2 = a(1-aF) \tag{4-8}$$

where ***a*** is axial flow induction factor, ***b*** is circumference flow induction factor, ***r*** is the radius of the blade element, $\lambda_r^2 = \pi\varpi_r / 60u$ is tip speed ratio of a blade element of radius equal to ***r.F*** is

Prandtl tip loss coefficient can be defined as

$F = \frac{2}{\pi}\arccos(e^{-f})$ where the parameter f can be expressed as

$$f = \frac{B}{2}\frac{R-r}{R\sin\phi} \qquad (4\text{-}9)$$

where ***B*** is the number of blades, ***R*** =D/2 is the radius of the rotor and ϕ is the fluid inlet angle [36].

The fluid inlet angle ϕ is determined by $\phi = \arctan\frac{(1-a)u}{(1+b)\omega_r} = \arctan\frac{1-a}{1+b}.\frac{1}{\lambda_r}$, The twist angle

$$\beta = \phi - \alpha \qquad (4\text{-}10)$$

The axial flow induction factor ***a*** and circumference flow induction factor ***b*** can be defined as

$$a = \frac{1}{\frac{4F\sin^2\phi}{\alpha C_n}+1} \text{, but } C_n = C_L\cos\phi + C_d\sin\phi \qquad (4\text{-}11)$$

and b is determined from the relation in the above equation which is $b(1+b)\lambda_r^2 = a(1-aF)$ and the length of chord line at the section of radius equal to ***r*** can be defined as

$$c = \frac{8\pi\sin^2\phi(1-aF)arF}{BC_L\cos\phi(1-a)^2} \qquad (4\text{-}12)$$

To examine the performance of the blade after sizing and defining geometry, it is important to study the relevant parameter as presented below.

The power coefficient and drag coefficient equation is required

Power coefficient C_P,

$$C_p = \frac{P}{\frac{1}{2}\rho V^2 A} \qquad (4\text{-}13)$$

Drag coefficient C_d can be determined from the following relation and using equation (3.15) as follows.

The rotor torque ***T***

$$T = \frac{1}{2}\rho_w A_T V^2 R \qquad (4\text{-}14)$$

and the torque coefficient is given by

$$C_T = \frac{2T}{\rho_w A_T V^2 R} \tag{4-15}$$

So, the drag coefficient can be computed from the following relation

$$C_T = C_L \sin\phi - C_d \cos\phi \tag{4-16}$$

The blade geometry is generated from NACA S1020 and the optimized profile is determined using the above formulas in an excel spreadsheet. The parameters used to optimize and size the blade geometry are chord length, Tip speed ratio at each section of the blade, fluid inlet angle ϕ, blade setting angle β, and Tip speed ratio on the entire blade determined using the equation (4-4), (3-5). (3-6), (3-9) respectively and presented in table 3.7. The power coefficient, torque, torque coefficient, and drag coefficient were determined using equations (4-17) to (4-18) and the result is shown in table 3.7.

Table 4-8 Aerodynamic design parameters

Parameters	***Value***
Power coefficient Cp,	0.45
Torque T	287.3163
Torque coefficient CT	1
Lift coefficient @ design point C_{ld}	1.1643
Drag coefficient CD	0.00793

Table 4-9 Turbine blade geometry generating data

Sec.No.	***Sect. radius r (m)***	λ_r	β	ϕ	***Chord length (m)***
1	0.1374	1.4	25.74367833	30.74368	0.072759359
2	0.2061	2.1	18.15170904	23.15171	0.062540672
3	0.2748	2.8	13.31203598	18.31204	0.052435526
4	0.3435	3.5	10.05452341	15.05452	0.044421824
5	0.4122	4.2	7.743269672	12.74327	0.038257303
6	0.4809	4.9	6.029791206	11.02979	0.033472133
7	0.5496	5.6	4.713614517	9.713615	0.029689551
8	0.6183	6.3	3.673196697	8.673197	0.026641815
9	0.687	7	2.831251495	7.831251	0.024142292

4.1.3 3D model of the blade using solid work

NACA S1020 is generated from the NACA series generator and it has to be the size of the chord length of the hydrofoil multiplied by each coordinate of the foil profile with design chord length using an excel spreadsheet but not change its sense of profile.

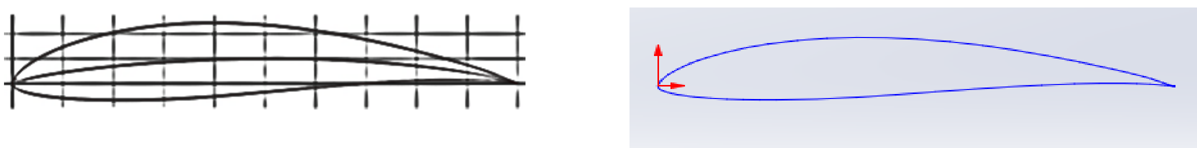

A) B)

Figure 4-5 A) airfoil curves from NACA series generator B) airfoil curves with the design size

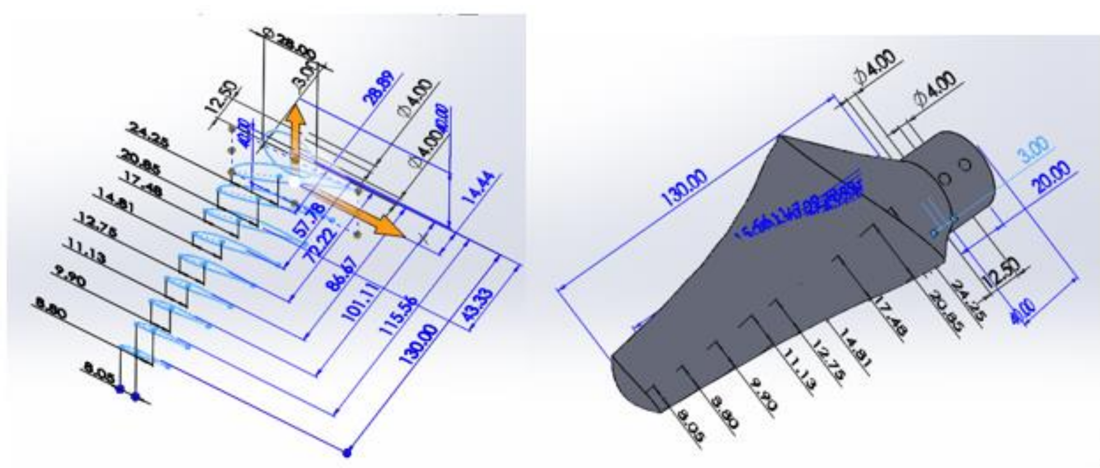

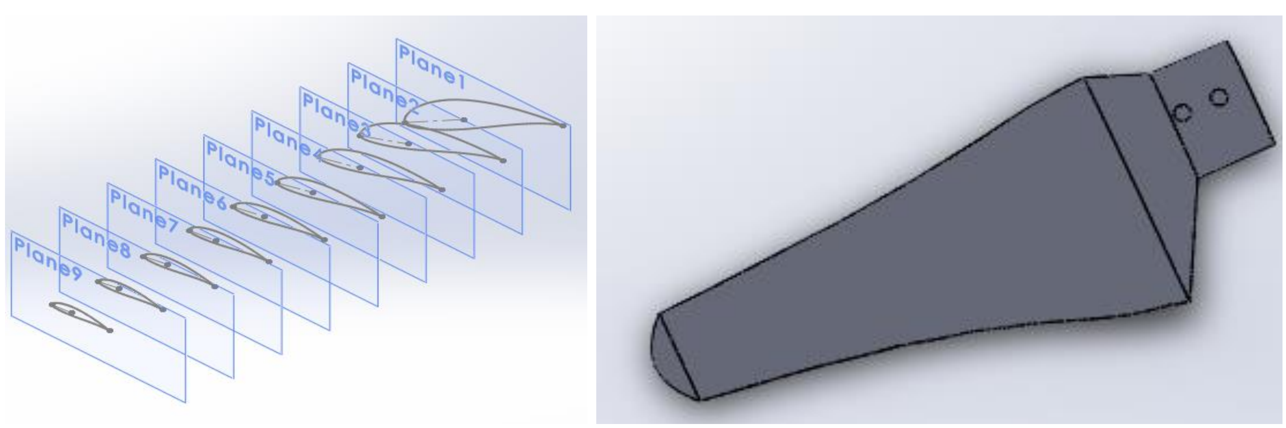

(A) (B)

Figure 4-6 (A) Airfoil curve construction and (B) Elemental blade

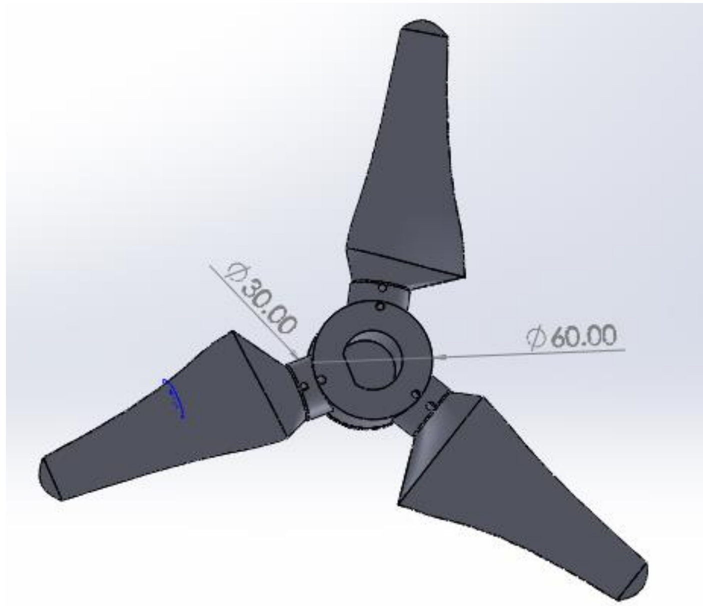

Figure 4-7 3D model of assembled blades

4.2 Flow simulation and force determination of blade using CFD

In general, there are two forces and one moment that act upon an airfoil; these being lift, drag, and pitching moment. The definitions of those three forces are explained in this section. Lift is the force used to overcome gravity and is defined to be perpendicular to the direction of the water flow. It is formed as a consequence of the unequal pressure on the upper and lower airfoil surfaces.

The drag force is defined as a force parallel to the direction of incoming water flow. The drag force is due both to viscous friction forces at the surface of the hydrofoil and to unequal pressure on the hydrofoil surfaces facing toward and away from the incoming flow. The lift is the force used to overcome gravity and the higher the lift the higher the mass that can be lifted off the ground [52].

Lift force, $F_L = \frac{1}{2} C_L \rho V^2 c$ (4-19)

Drag force, $F_D = \frac{1}{2} C_D \rho V^2 c$ (4-20)

Pitching moment, $M = \frac{1}{2} C_M \rho V^2 c^2$ (4-21)

Where $\boldsymbol{\rho}$ is the air density and $\boldsymbol{c}$ is the length of the airfoil, often denoted by the chord.

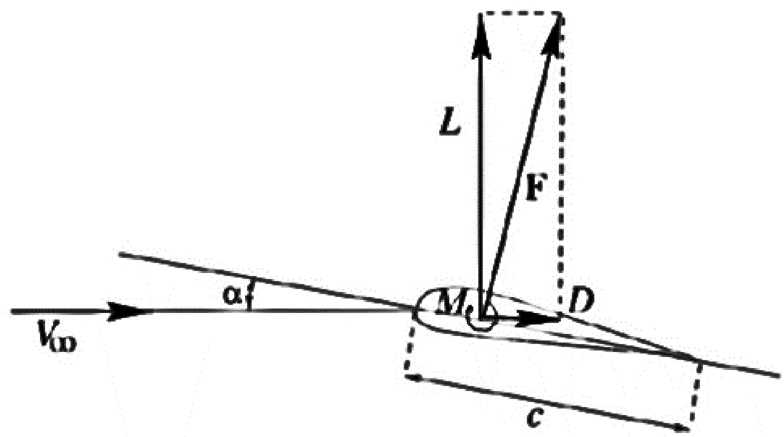

Figure 4-8 Lift & Drag force diagram[53]

While CFD simulations can generate accurate results, they can also be very time-consuming. In the conventional definition of a converged solution, two conditions must be met: the maximum normalized residuals of all solved equations should decrease seven orders of magnitude and all monitored quantities should not change with subsequent iteration. These conditions make the proposed optimization scheme very time-consuming due to the number of simulations required, even when high-performance computing resources are available. To decrease the computational time needed to run the simulations, a less strict convergence criterion is used. CFD simulations are run until they converge well enough to get a good estimate of the optimization output quantities such as the lift and thrust produced by the turbine blades [53].

The design parameters are calculated as per formulas used in the design of the blade. In this thesis, we consider the S1020 profile of the blade and 9 sections of the blade for the good consideration of the result. The main aim of the simulation is to identify the maximum pressure distribution on the surface of the blade to get sufficient lift force to rotate the turbine.

The process of CFD

1. Formulation of flow problem analysis approach is steady flow condition

The geometric model and file format is a step file and the imported file is shown in figure 3.14.

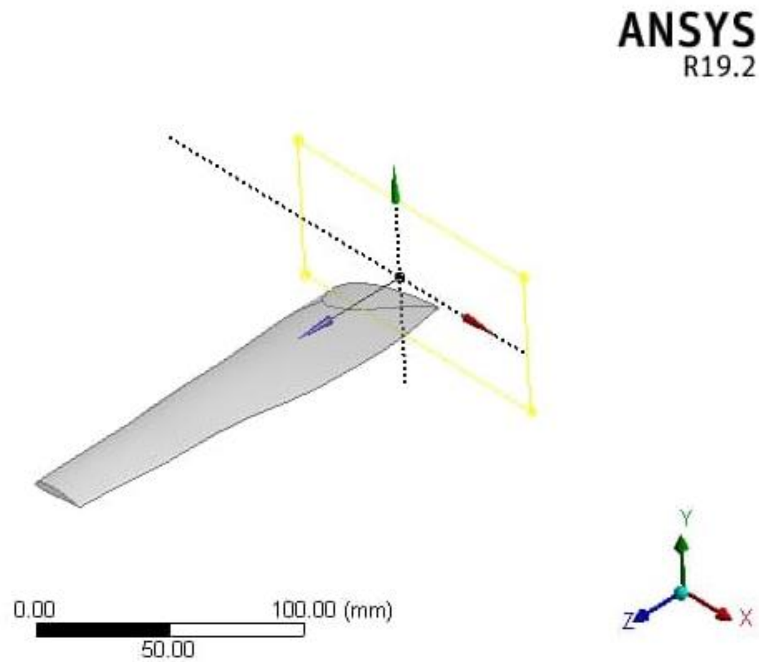

Figure 4-9 Geometric model of blade

2. Model the flow domain is the control volume (bounded by the control surface) in which the flow field is computed. The body is part of the surface of the flow domain.

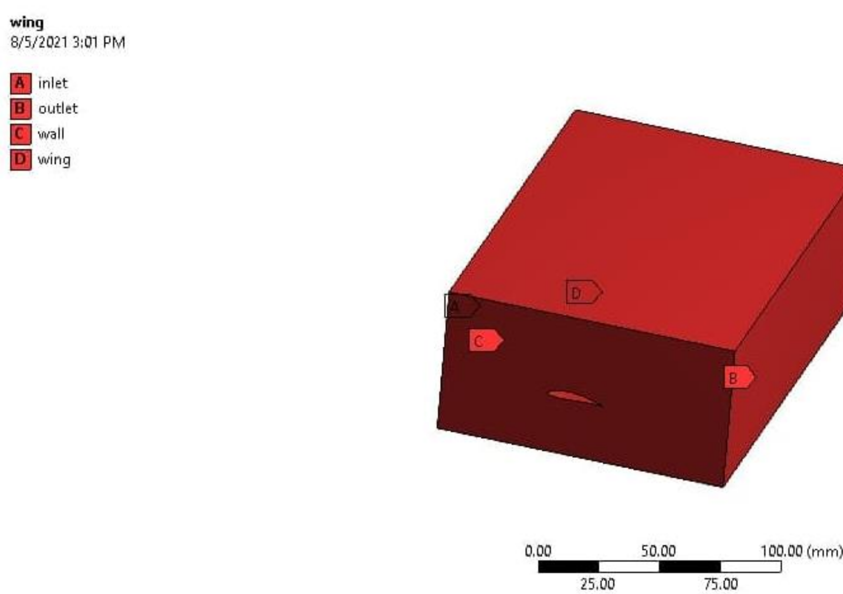

Figure 4-10 flow domain geometry

3. Generate the grid

A grid is generated within the flow domain. the grid consists of finite-volume cells on which the CFD equations are approximated. The simulation requires precious meshing of the object to get an accurate result so, we made the mesh with the required properties. We use for this simulation,

The Control domain size is x length of 0.1351m, y length 5.0732e-002 m and its volume are 1.0058e-003 m^3.

Sizing of mesh

Quality of mesh: Smoothing High

Inflation:

- ✓ Inflation Option Smooth Transition
- ✓ Transition Ratio 0.272
- ✓ Maximum Layers 5
- ✓ Growth Rate 1.2

Element Size **1.0938e-002**, the number of node and mesh elements are **272301** and **1488071** respectively.

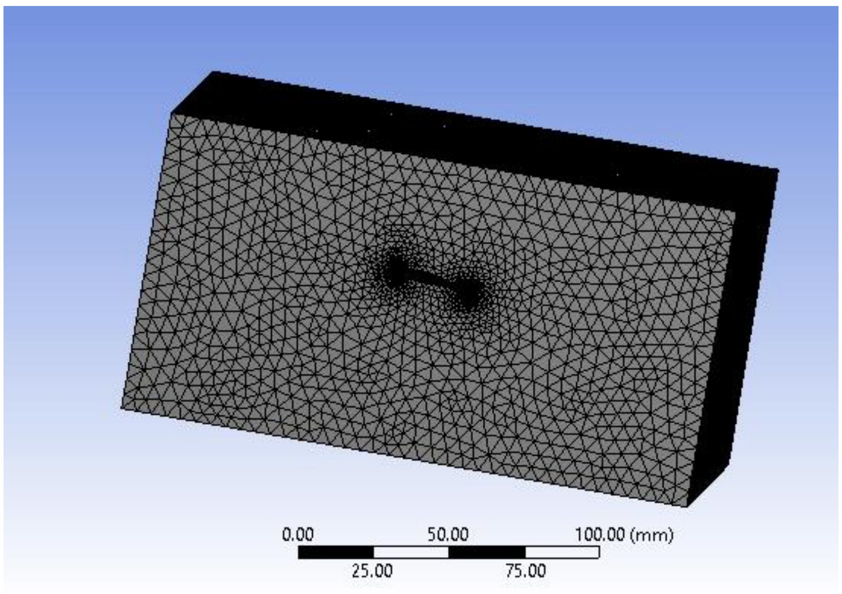

Figure 4-11 Meshed model

4. Specify the boundary and initial condition

The Environment domain type and fluid type is water that all consider parameter in Ansys 19.2

- ✓ Fluent, also we define the inlet and outlet parameters in the geometry.
- ✓ The measured velocity of the water of the river is 0.75m/s
- ✓ The pressure velocity scheme is considered as simple with spatial discretization gradient is least-squares based and water momentum is to be Second order upwind.
- ✓ Defining all boundary conditions,
- ✓ The turbulence model adopted for this study is the Realizable k−ε model: it is more accurate for predicting the speeding rate of both planar and round jets but it will produce non-physical turbulent viscosities when the simulated model includes both rotating and stationary fluid zone[54].

5. Examine and process the result

Finally, the solution is initialized from the inlet and starts the calculations with 1600 iterations and the simulation is converged.

6. Report the result

The results of the CFD simulation were represented and discussed in the results and discussions section.

4.3 Sizing of mechanical components

The mechanical components of the hydrokinetic turbine for this purpose are Shaft, gearbox, hub, and floating device. As presented in the conceptual design section the arrangement of the hydrokinetic turbine is a horizontal axis turbine. But to change the direction of rotation of the horizontal axis shaft to the vertical direction requires to use of bevel gear inside the gearbox and getting the required power on the given orientation of the hydrokinetic turbine. From the design concept, this bevel gear is complex and difficult to manufacture locally as result it is better to use a belt drive mechanism for the desired orientation of hydrokinetic turbine. It is a simple mechanism and easy to design and can be driven by simple power to generate electricity to meet the objective of this study.

To design the drive the first task is to identify relevant types of the belt which are made of different materials.

Cotton or fabric belts: most of the fabric belts are made by folding canvas or cotton duck to three or more layers (depending upon the thickness desired) and stitching together. These belts are woven also into a strip of the desired width and thickness. They are impregnated with some filler like linseed oil to make the belt water-proof and to prevent injury to the fibers. The cotton belts are cheaper and suitable in warm climates, damp atmospheres, and exposed positions. Since the cotton belts require little attention, therefore these belts are mostly used in farm machinery, belt conveyors [55]. So, this hydrokinetic turbine operated by water the belt must be waterproof material which is made by cotton.

The types of the belt based on configuration are open belts depending on this arrangement the pulley was designed using the design specifications.

Specifications are as follows depending on the depth of the water and the size of the turbine blade to keep its proportionality.

Pulley diameters for small & large pulleys are 30mm & 200mm respectively
The gap between two centers of pulley X= 450mm
Groove angle =17
Input speed N_1=73.012 rpm
Power transmitted by pulley P= 250W

Based on those specifications firstly need to determine the output speed using velocity ratio and consider the slip condition for both pulley S=1.2%

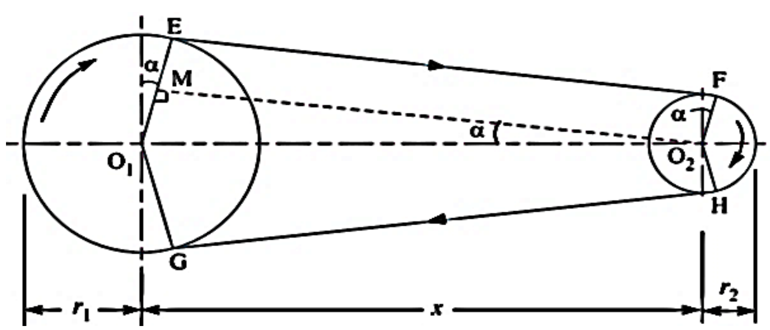

Figure 4-12: pulley layout [55]

The velocity ratio is without considering belt thickness

$$\frac{N_2}{N_1} = \frac{D_1}{D_2}(1 - s/100) \tag{4-22}$$

Then from this relation, we can determine the output speed of the pulley

$$N_2 = \frac{N_1 \times D_1}{D_2} = \frac{73.012 \times 200}{30} = 486.75rpm$$

The peripheral velocity of the belt evaluated under slip condition which is

$$V_1 = \frac{\pi \times D_1 \times N_1}{60}(1 - s/100) \qquad (4\text{-}23)$$

$$V_1 = \frac{\pi \times 200 \times 73.012}{60}(1 - 1.2/100) = 0.755m/s$$

And $V_2 = \frac{\pi \times D_2 \times N_2}{60}(1 - s/100)$

$$V_2 = \frac{\pi \times 30 \times 486.75}{60}(1 - 1.2/100) = 0.755m/s$$

For the open belt drive, the length of the belt can be determined using the formula

$$L = \frac{\pi}{2}(D_1 + D_2) + 2X + \frac{(D_2 - D_1)^2}{4X} \qquad (4\text{-}24)$$

$$L = \frac{\pi}{2}(0.2 + 0.03) + 2 \times 0.45 + \frac{(0.2 - 0.03)^2}{40.45} = 1.277m$$

The angle of contact between the belt and each pulley

$\theta = 180^0 + 2\alpha$ but, $\sin\alpha = \frac{r_1 + r_2}{x} = \frac{0.1 + 0.015}{0.45} = 0.2555, \alpha = \sin^{-1}(0.2555)$

$\alpha = 16.45^0$

Then, $\theta = 147.1$, and with radian measure $\theta = 147.1 * \frac{\pi}{180} = 2.5661$

Power transmitted by the belt taking the ratio of tension for the tight and slack side of the belt

Table 4-10 Coefficient of friction between belt and pulley and its belt material density[55]

Belt material	***Pulley material (coefficient of friction)***			***Mass density(kg/m³)***
	Rubber face	***Compressed paper***	***wooden***	
Cotton woven	0.3	0.28	0.25	1170
Rubber	0.42	0.35	0.32	1140
Balata	0.42	0.38	0.35	1110

$$2.3\log(\frac{T_1}{T_2}) = \mu\theta \quad (4\text{-}25)$$

$$2.3\log(\frac{T_1}{T_2}) = 0.3*2.5661 = 0.77 \;,\; (\frac{T_1}{T_2}) = 1.08$$

Taking the maximum permissible tension T_1 =500N in most designs for small-scale purposes[55].

$$T_2 = \frac{500}{1.08} = 462.963N$$

The centrifugal tension is not considered because of the velocity of the belt below 10m/s. there is no effect below this velocity[55].

4.3.1 Design of shaft and pulley

We know that the torque transmitted by the driven pulley

$$T = \frac{design\ \text{power} \times 60}{2\pi N_2} = \frac{250*60}{2\pi*486.75} = 50N.m = 50,000N.mm$$

Since the overhang of the pulley is ***250 mm***, therefore bending moment on the shaft due to the belt tensions and there is no Tc under this condition therefore the bending moment is

$M = (T_1 + T_2)*overhunging*n$ where T_1 & T_2 are tension tight and slack side of the belt and n is the number of belts here for this design case n=1

$$M = (500 + 462.963)*250*1 = 240.74*10^3\,N.mm$$

The equivalent twisting moment is T_e

$$T_e = \sqrt{T^2 + M^2} \quad (4\text{-}26)$$

Because the shaft is subjected to bending and twisting moment

$$T_e = \sqrt{(50*10^3)^2 + (240.74*10^3)^2} = 245.878*10^3\,N.mm$$

And also, we know that the equivalent moment has an expression

$$T_e = \frac{\pi}{16} * \tau * D^3 \quad (4\text{-}27)$$

but the ultimate tensile strength 615 Mpa [55]

And the permissible shear stress is $\tau = \sigma_u * 0.18 = 615 * 0.18 = 110.7 Mpa$

Then the shaft diameter determines from this relation

$$D = \sqrt[3]{\frac{T_e * 16}{\tau * \pi}} = \sqrt[3]{\frac{245.878*10^3 * 16}{110.7*10^6 * \pi}} = 22.5mm$$

4.3.2 Design of pulley

The dimensions for the standard *V*-grooved pulley are A-type depending on the following table.

Table 4-11 Types of belts [55]

Types of belts	***Power (kW)***	***Groove angle***	***f (mm)***	***e (mm)***
A	0.7-3.5	32,34,38	10	15
B	2-15	32,34,38	12.5	19
C	7.5-75	34,36,38	17	25.5
D	20-150	34,36,38	24	37

Using the above standard can determine the face width of the pulley no need for the detailed design of the pulley because it can take from standard.

Therefore, the face width, $B = (n-1)e + 2f$

$B = (n-1)e + 2f = (1-1)15 + 2*10 = 20mm$ because the number of the belt (n) is 1

4.4 The manufacturing process of the turbine blade and its mechanical components

Increased automation technology in the wind turbine manufacturing process is a laborious alternative and requires substantial financial investment, but it achieved simplicity, economy and increases the final quality of each turbine. Increased reliability and cost optimization are top priorities for improving the competitiveness of the wind energy sector in an increasingly competitive international environment[56].

The hydrokinetic turbine is analogous to the wind turbine in its design procedures, working principles, and manufacturing processes. As mentioned earlier the difference is operating fluid. The manufacturing technology was upgraded from time to time and now this technology brings 3D print technology for every product with high precision as well as effective production time.

Digital fabrication technology, also referred to as 3D printing or additive manufacturing, creates physical objects from a geometrical representation by successive addition of materials. 3D printing technology is a fast-emerging technology. Nowadays, 3D Printing is widely used in the world. 3D printing technology is increasingly used for mass customization, production of any type of open-source designs in the field of agriculture, healthcare, automotive industry, locomotive industry, and aviation industries.

3D printing technology can print an object layer by layer deposition of material directly from a computer-aided design (CAD) model. explain the types of 3D printing technologies, the application of 3D printing technology, and lastly, the materials used for 3D printing technology in the manufacturing industry [57]–[60] 3D printers have many promising areas of potential future applications.

New 3D printing processes have reduced the time it takes for designers and engineers to conceptualize, create, and test prototypes. But for 3D printing to catch on to the rapidly changing manufacturing industry, it will have to be seen by companies less as a fascinating technological upgrade and more as an everyday business decision. Some of the most promising areas include medical applications, custom parts replacement, and customized consumer products[61]. Comparatively, 3D printing technology is suitable for manufacturing the blade for this study from other manufacturing methods. Therefore, the hydrokinetic turbine blade was manufactured using a 3D printer.

The material used for manufacturing this hydrokinetic turbine blade is polylactic acid (PLA). The polymer, polylactic acid, polylactide, or more commonly known by its abbreviation PLA, versatile polymer. PLA is biodegradable and exhibits thermoplastic behavior. While PLA has modern industrial uses, including textiles and packaging. The innate characteristics of PLA lend themselves to rapid prototyping and efficient manufacturing in 3D printed constructs. PLA consists of lactic acid monomers which compose its polymeric backbone.

PLA may also refer to as 2-hydroxy propionic acid or cyclic diester lactide. The first recorded synthesis of PLA was in 1932 by Wallace Carothers at Dupont laboratories. Since then, the usage of PLA has expanded greatly. In 2016, the bioplastic market has experienced an 11% annual increase generating a revenue of more than 2.6 billion USD.

Engineers and scientists have capitalized on the many applications of this material advantage. Such advantages are environmentally friendly, easy production, recyclable, compostable, biocompatible, and few no reported carcinogenic effects. PLA may be derived from renewable resources such as carbon dioxide, wheat, corn, and rice. PLA degradation products are also non-toxic to humans and the environment. PLA uses 25-55% less energy to produce than petrol-based polymers[62].

Mechanical properties of PLA

Mechanical properties of PLA may vary given the molecular weight of polymer and degree of crystallinity. Mechanical properties are also governed by the stereochemical configuration of molecular structures of the PLA backbone. Given that lactide monomers are chiral, mechanical properties can be manipulated through the polymerization of D-lactide, L-lactide, or meso-lactide. The molecular weight may also be changed through the addition of functional groups to the backbone.

These functional groups may include the addition of hydroxyl species, lactic acid, and water. As a result, the user may modify the configurations of the PLA polymer backbone to achieve the desired properties. Improved mechanical properties of PLA can be achieved with semi-crystalline PLA over an amorphous assemble of the polymer. So PLA is an advantageous biopolymer with relatively high strength and high modulus [62]

Table 4-12 Mechanical properties of PLA[62]

S. No	Characteristics	Amount
1	Tensile modulus	3Gpa
2	Tensile strength	50-70Mpa
3	Flexural modulus	5Gpa
4	Flexural modulus	100Mpa

Table 4-13 physical properties of commercialized PLA[62]

S.No.	***Characteristics***	***Unit***	***Amount***
1	Molecular weight	g/mol	66000
2	Specific gravity		1.27
3	Solid density	g/cm^3	1.252
4	Melting density	g/cm^3	1.073
5	T_g	^0C	55
6	T_m	^0C	165
78	Specific heat	J/kg. ^0C	
9	190 ^0C		2060
10	100 ^0C		1955
11	55 ^0C		1590
12	Thermal conductivity	w/m. ^0C	
13	190 ^0C		0.195
14	109 ^0C		0.197
15	48 ^0C		0.111

As we have seen from the table above the density is very light and its strength and modulus are high comparatively. The main criteria to select the material for the production of the hydrokinetic turbine are density, availability, and its cost as well as its manufacturing ability to produce. Therefore, the vital material is selected PLA.

Production of PLA

Industrial lactic acid production utilizes the lactic fermentation process rather than synthesis because the synthetic routes have many major limitations, including limited capacity due to the dependency on a by-product of another process, inability to only make the desirable L-lactic acid stereoisomer, and high manufacturing costs. The homofermentative method is preferably used for industrial production because its pathways lead to greater yields of lactic acid and lower levels of by-products.

PLA production steps by ring-opening polymerization using stannous octoate as an initiator. New ideas for decreasing PLA final price and making production processes eco-friendlier, in comparison to the earlier production process, including the usage of crop residue namely stems, straw, husks, and leaves from corn or, potentially, other crops, and use of unfermentable residues as a heat source, as well as substituting some part of electrical energy by wind power energy. These approaches decrease the consumption of fossil fuels and corn starch as raw materials and also minimize polluting air, water, and waste emissions to the environment. One of the most positive points of PLA production in comparison with the other hydrocarbon-based polymers is the decrease in CO_2 emissions.

Carbon dioxide is believed to be the most important contributor to global climate change and its warming. Because carbon dioxide is absorbed from the air when corn is grown, the use of PLA has the potential to emit fewer greenhouse gases compared to competitive hydrocarbon-based polymers. Net or residual emissions are calculated as total emissions from the cradle to the factory gate minus carbon dioxide uptake that occurs during corn production. This amount is negative for present PLA production. It means the total CO2consumption from the cradle to the factory is more than its emission to the environment. Vink et al. (2003) concluded if all produced PLA articles enter into composting process which emits CO2 in the atmosphere; Nevertheless, their net CO2 emissions are less than for other polymers [63]. The 3D print turbine is shown in figure 4.13

Figure 4-13 3D Printed turbine blade

Manufacturing of mechanical components

The mechanical components are the motor, stand, and transmission components. The transmission components are shaft, pulley, bearings, and cotton belt.

This manufacturing process is not complicated simply welding, cutting, and turning in the mechanical workshop. The motor stand(frame) is manufactured from a rectangular hollow section metal (RHS) by cutting and welding and the motor is also welded over the stand. There is a bed to support the bearing and shaft. Turning of shaft diameter to get the design size of the required diameter. The rest bearings and pulley were already purchased from the market with the specified dimension. The pulley was taken from an old laundry machine and its material was also plastic. The cotton belt is prepared by rolling the cotton fiber and it is lightweight. All the components are shown below in figure 4.15. The manufacturing flow diagram of the turbine.

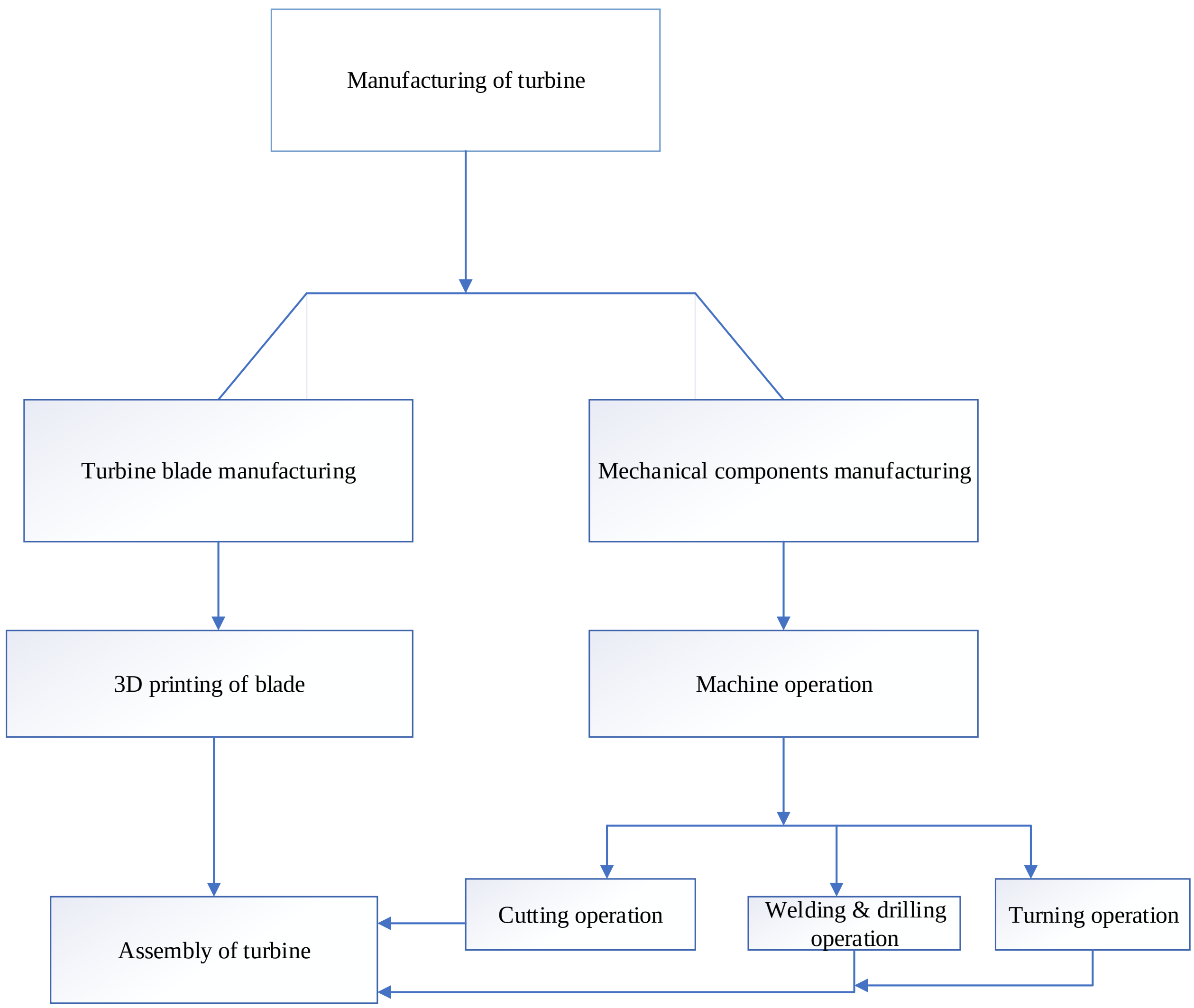

Figure 4-14 Manufacturing process of turbine

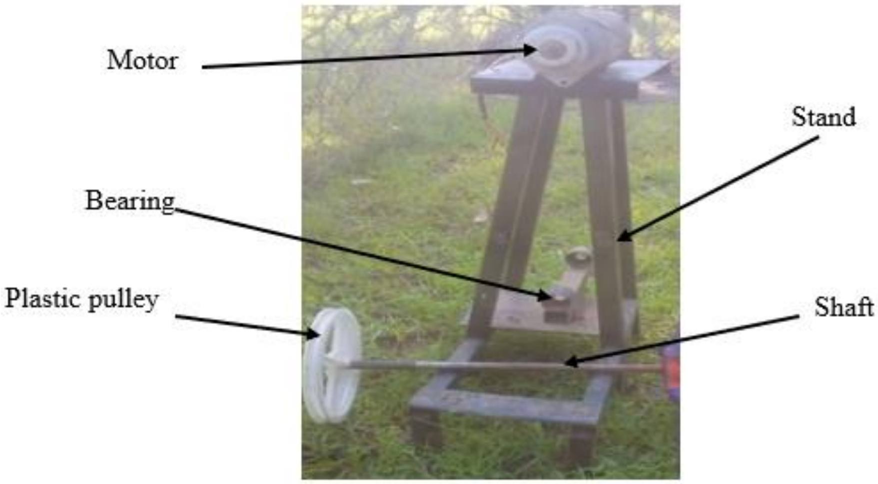

Figure 4-15 Manufactured of mechanical components

4.5 Experimental setup

The experimental setup was developed to measure the amount of AC power generated by the hydrokinetic turbine. The overall assembly of the turbine and another measurement (electrical equipment) are required to conduct the test. For a better result recording oscilloscope is more accurate but we use only multi-meter and phone camera as we can get them easily. A tachometer is also used to measure the rpm of the motor driven by the turbine as a result of the kinetic energy of the water. Supportive materials used in this setup are electrical wire, small(<9w) bulb, meter and, floating element. The turbine, river and, multimeter with the bulb is shown in figure 4.16

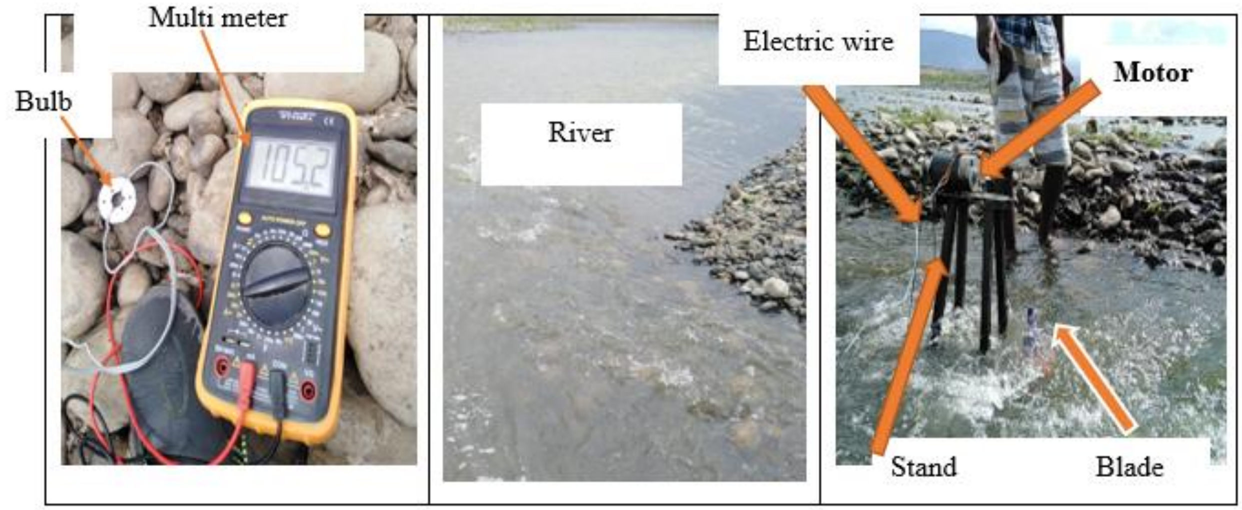

Figure 4-16 Experimental apparatus and turbine in the river

The test was done by placing the turbine into the river the blade is submerged in the water but the motor is free from water contact for the sake of preventing the motor from any damage.

As mentioned in the design section, the velocity of water measured is 0.75m/s. the first test was done in the hydraulics lab and there are two channels for the test but both of the channels are having a low velocity. The value is 0.0325m/s is for the bed cannel and the narrow channel is unmeasurable because it is turbulence flow but the value greater than the wide channel with a simple observation. The test in the lab indicates the velocity of the narrow channel is below the design velocity because it does not run the turbine using that flow of water. The next step is to try to minimize the mass of mechanical components of the turbine which are turning shaft diameter and pulley mass and its types of material which is the plastic pulley.

A) Wooden pulley turbine   B) Plastic pulley turbine

Figure 4-17 Hydrokinetic turbine with wooden pulley

After the above work has been completed, the goal of the experiment is not a chivied and another option is needed to change the type of pulley material and increase the diameter of the input pulley. An aluminum pulley with 140mm diameter and 340.723rpm of the motor can achieve the maximum value of voltage 5.27V but there is no current displaying on the multimeter. Then to get the required current output tried to increase its pulley diameter again.

The plastic pulley with a diameter of 200mm was taken from an old washing machine. The turbine then reassembles and takes into the river. Finally, the results are getting as we expected and all the results getting from the experiment are discussed in detail in the result and discussion section of the report.

The plastic pulley has a diameter of 200mm and the rpm increase from 340.723rpm to 486.75 rpm and within this rpm, the motor can extract the maximum calculated power of 133.811 watts at maximum voltage and AC 9.69 V and 16.03 Amp respectively and it can give light to the bulb as shown on the figure 3.31 below.

The AC and voltage display using the oscilloscope is a sinusoidal pattern represented on the graph AC and voltage versus time. The recording of this data on this experiment manually as soon as possible and the result is having sinusoidal pattern but the amplitude is not equal in each recording time because of the production accuracy of mechanical components and lack of digital measurements.

Basic electricity concept to analyze the experiment results

The results fit with theoretical science and the difference was the performance of the hydrokinetic turbine due to some mechanical production quality loss.

If negative values of voltage and alternating current encounter the source of voltage change polarity periodically and the negative and positive sign indicates the direction of current flow. The signs of alternating current are allocated for a reference direction given on the circuit diagram. This time-dependent voltage and current are expressed mathematically and can also express the generated power based on the relation of voltage and alternating current to the power.
The Source of AC is a coil of wire rotating with constant angular speed (ω) in a magnetic field for sinusoidal alternating emf. And having the mathematical model represented as a function of time [64]

$$I(t) = i\cos\omega t \qquad (4\text{-}28)$$

$$V(t) = v\cos\omega t \qquad (4\text{-}29)$$

$$P = V(t) * I(t) \qquad (4\text{-}30)$$

where I and i are time-dependent current and peak value of current respectively and V and v are also a function of time and peak value of voltage respectively. ω is the angular speed of coil wire and it is $\omega = 2\pi f$ [64].

When we introduce the phase angle ϕ of source voltage concerning current the voltage is expressed as $V(t) = v\cos(\omega t + \phi)$. Therefore, the power gives as

$$P = vi\cos\phi\cos^2\omega t - vi\sin\phi\cos\omega t\sin\omega t \qquad (4\text{-}31)$$

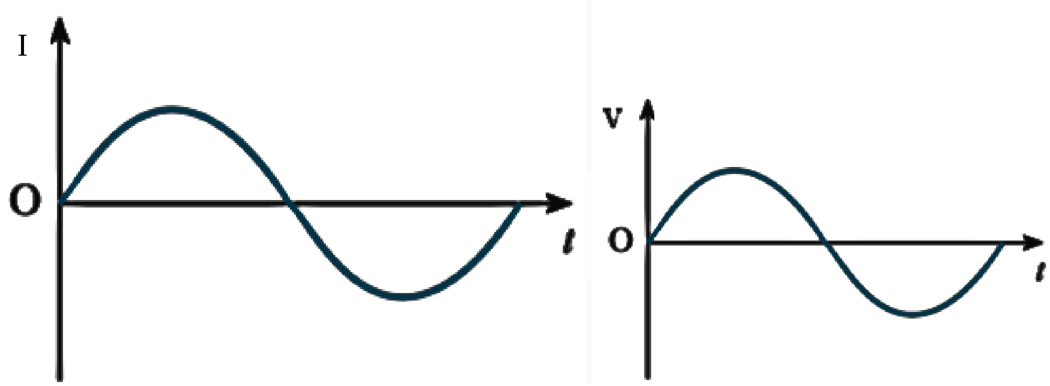

Figure 4-18 sinusoidal graph of AC voltage representation

As we have seen from the above graph the real case of generating AC, and voltage signals using an oscilloscope are sinusoidal patterns. The same is true for the experimental results of this work. But the results must represent the root mean square value of current and voltage to know generating capacity of the turbine.

Therefore, we can analyze the result reference with to this time-dependent graph pattern of current and voltage of the alternating current source.

The maximum instantaneous value of voltage measured from zero value is the peak value of voltage. Therefore, the maximum variation between the maximum positive instantaneous value and the maximum negative instantaneous value is the peak-to-peak value of voltage and represented by graph was positive value and the experimental results also indicates peak to peak value voltage.

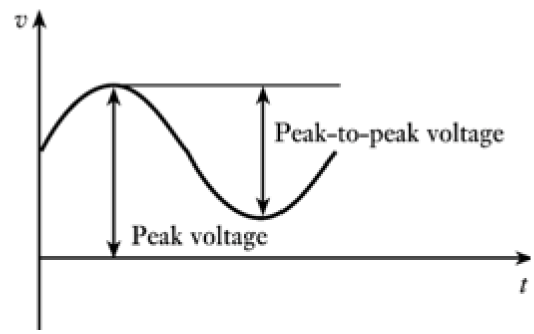

Figure 4-19 peak-to-peak values of voltage representation [65]

The relationship of power and torque are directly proportional shown from the mathematical model. The expression is $p = \frac{2\pi * NT}{60}$ (4-32)

Based on the expression we can get the torque of the motor to generate the resulting power.

$$T = {P*60}/{2\pi N} \quad (4\text{-}33)$$

The experiment in this study only measures the current and voltage using a multi meter. The power and torque are calculated values based on equations 3.31 and 3.34 because the instrument used to measure power and torque directly from the experiment is not available. The detail about these values is next in the results and discussions section.

Chapter 5: Results and Discussions

5.1 Flow simulation results and forces exerted on the blade

The results are converged as we have seen in figure 4.1 and all the detail velocity and pressure contour, as well as lift and drag forces, are discussed.

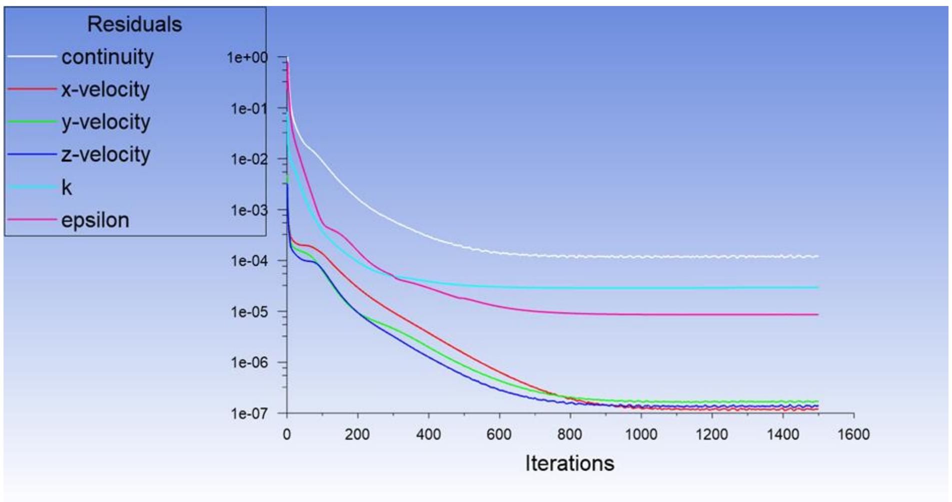

Figure 5-1 Residuals

The simulation is converged on the iteration of 1500 because the mesh size and methods

Mesh independent Test

A CFD solution can never be trusted unless we check whether the result depends on the grid or not. The output results of the coarser mesh and finer mesh can neither be the same. So, up to what extent do we need to vary the mesh to get the accepted level of tolerance. This is done by varying the mesh size from coarse to fine and checking the result for each mesh. When varying the mesh does not affect the result much then we can do our solution on that mesh size.

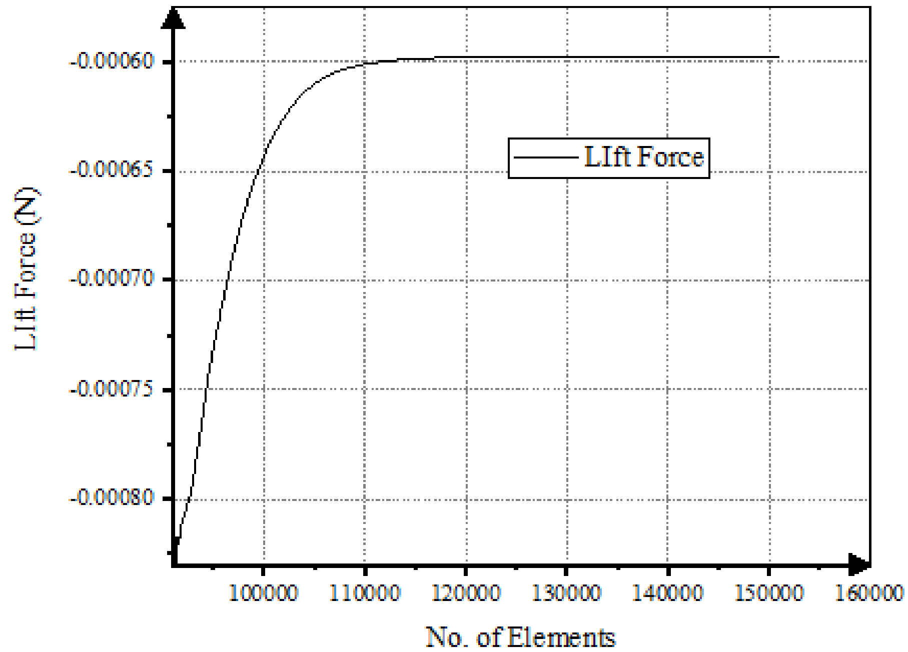

Figure 5-2 Mesh independent Test

The result variation is not significant after the number of elements of 1488071 and it is almost similar results beyond this number of elements. This mesh size gives accurate results with less time as compared to finer mesh.

Report the result

The result is shown below, the lift and drag force, lift and drag coefficient, and moment and moment coefficient plotted in figures 5.3 and5.4. The pressure distribution and velocity contour are presented in figures 5.5 to 5.10.

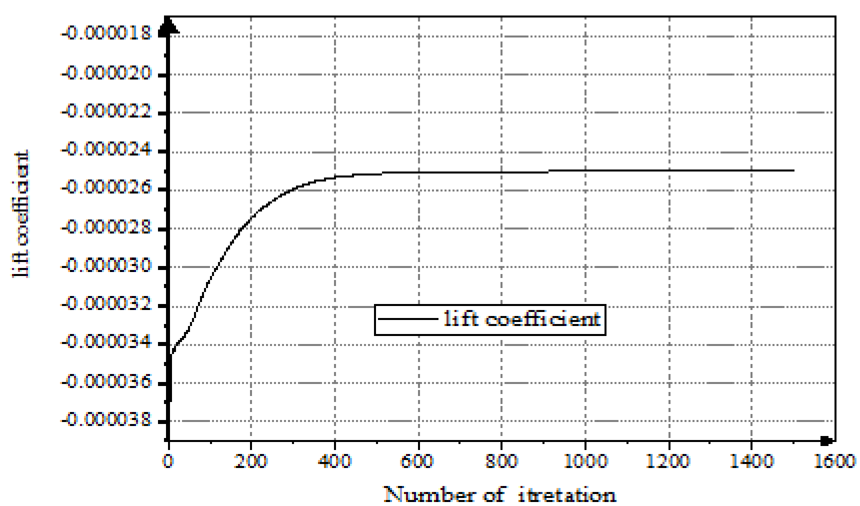

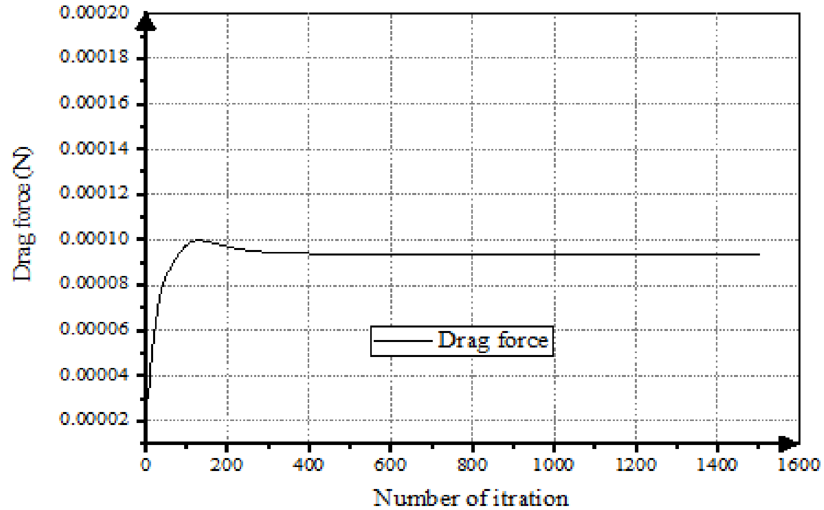

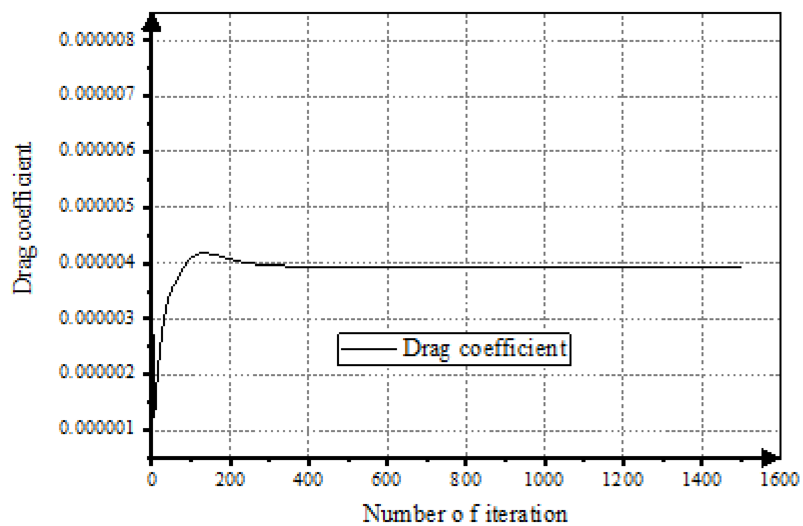

Figure 5-3 Lift force and Lift coefficient, drag force and drag coefficient convergence iteration

This convergence iteration shows the convergence of the computation result is accurate and it also shows the proper use of the fluent with stepwise applying of simulation.

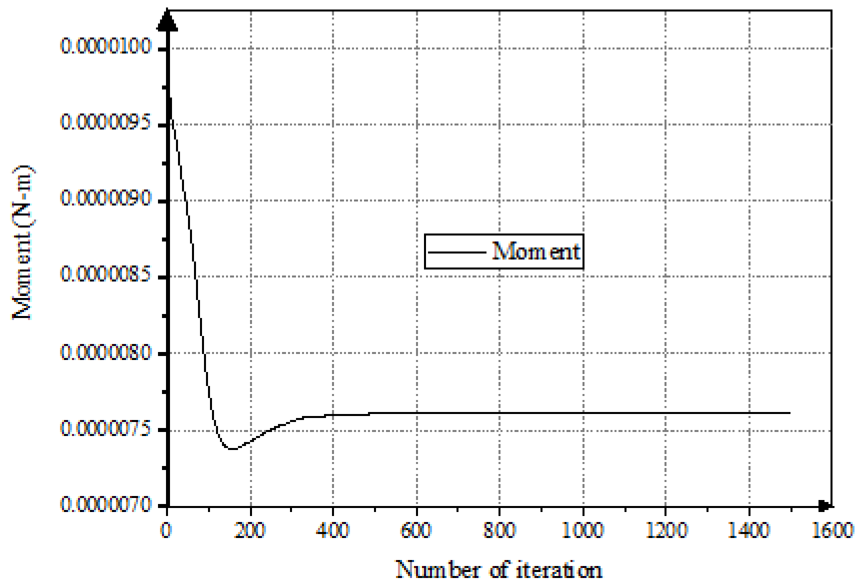

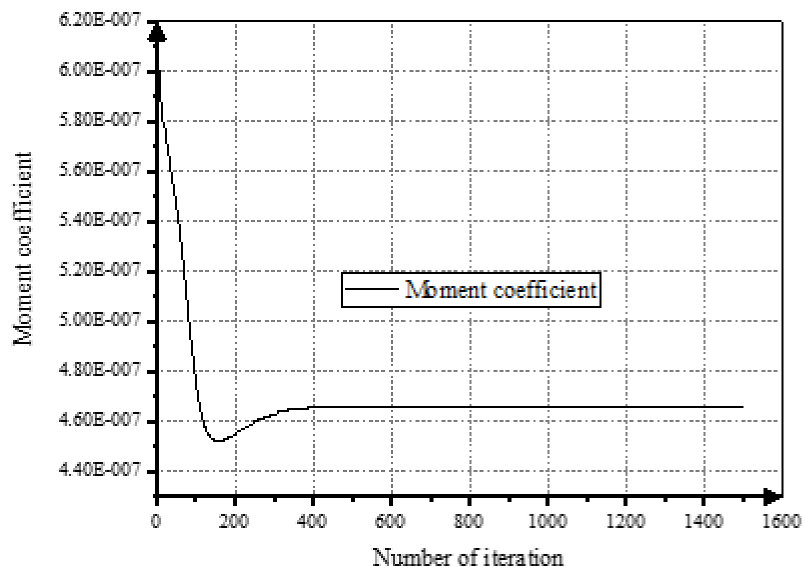

Figure 5-4 Moment and moment coefficient convergence iteration

The moment shows a low effect on the blade because the convergence results are minimum.

The resulting pressure distribution and velocity are generated from the computation of Ansys fluent 19.2 as follows.

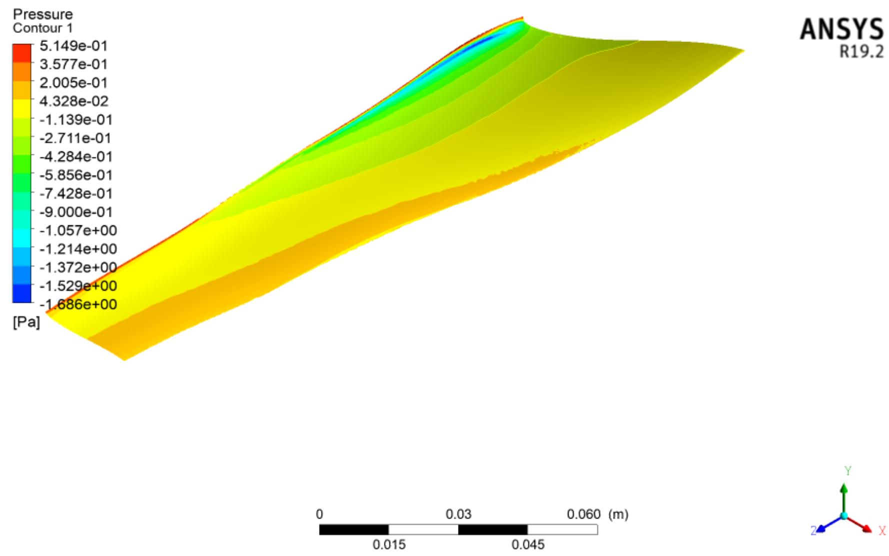

Figure 5-5 Pressure distribution on the blade

The pressure distribution indicates on the surface of the blade more on the lead edge of the blade and some exertion of pressure overall surface of the blade from the tip of the blade but there is a little surface free from the pressure to the tail of the blade (from the root of the blade).

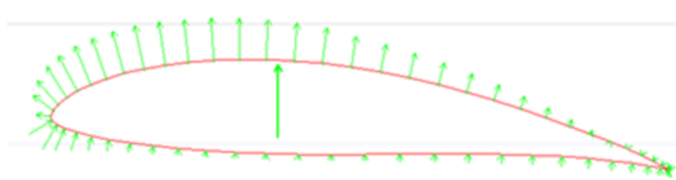

Figure 5-6 Pressure distribution of airfoil exported from QBlade software

As we have seen the 2D airfoil simulation using QBlade design software the maximum pressure distribution from the leading edge on the upper surface and minimum from the trailing edge.

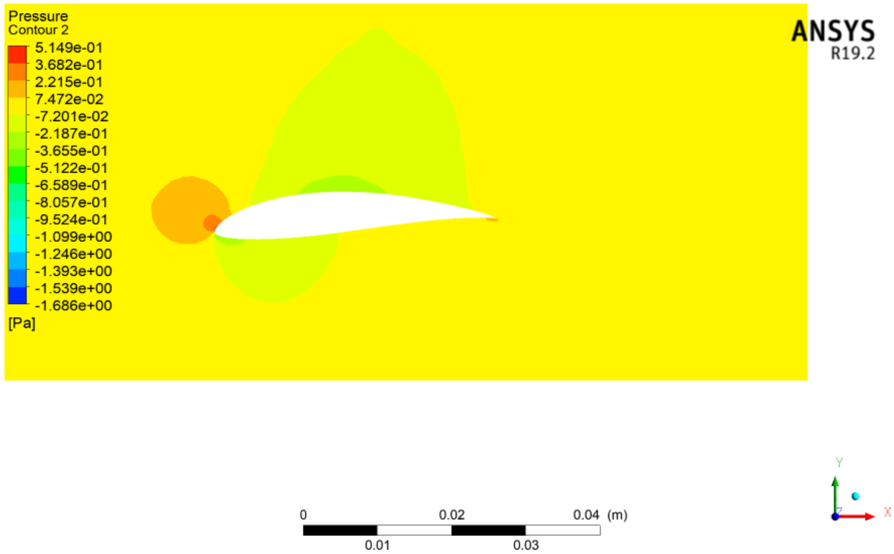

Figure 5-7 Pressure contour at 5^0

The pressure contour on airfoil high pressure develops on leading-edge from the upper surface of the airfoil and the trailing edge on the lower surface of airfoil moderate pressure developed and it have also sufficient lift to rotate the blade.

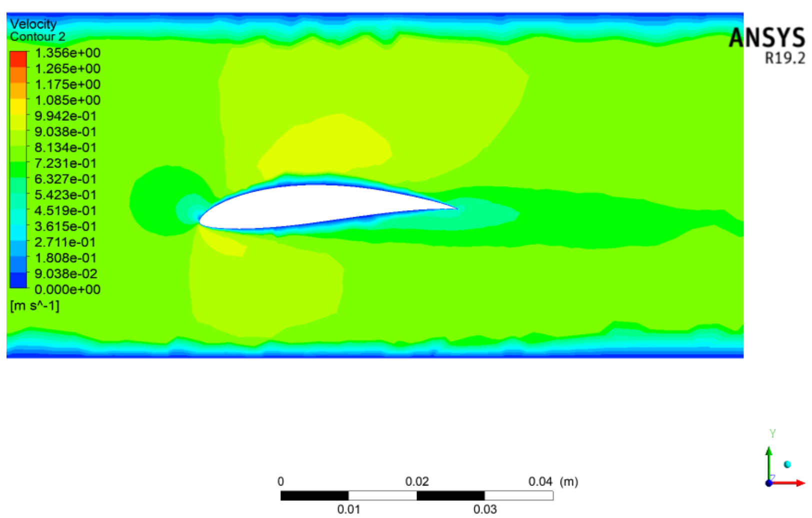

Figure 5-8 Velocity contour at 5^0

The velocity contour showed on the simulation result there is a good velocity flow on the upper surface at the maximum thickness and around it but this flow is not touching the surface. On the pressure concentration surface of the blade, the velocity is low and vis versa there is no wake and stall.

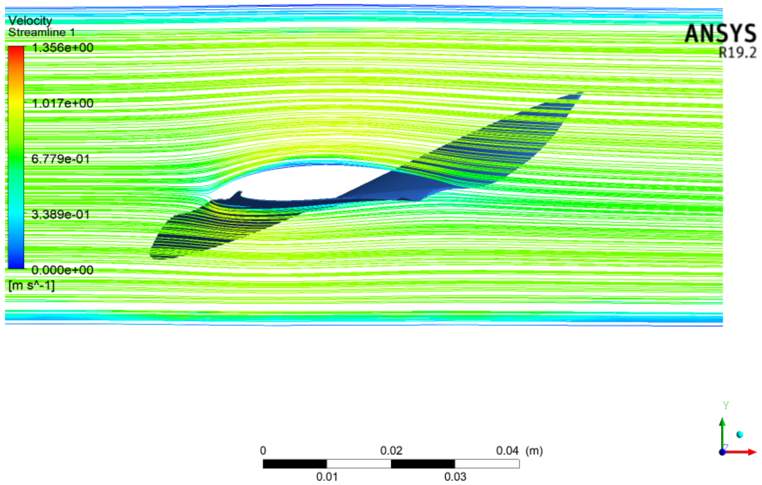

Figure 5-9 Streamline velocity

The streamline velocity shows there is no wake at the trailing edge of the airfoil and the incoming flow is fast over the upper surface of the airfoil and slow to the lower surface of the airfoil accordingly.

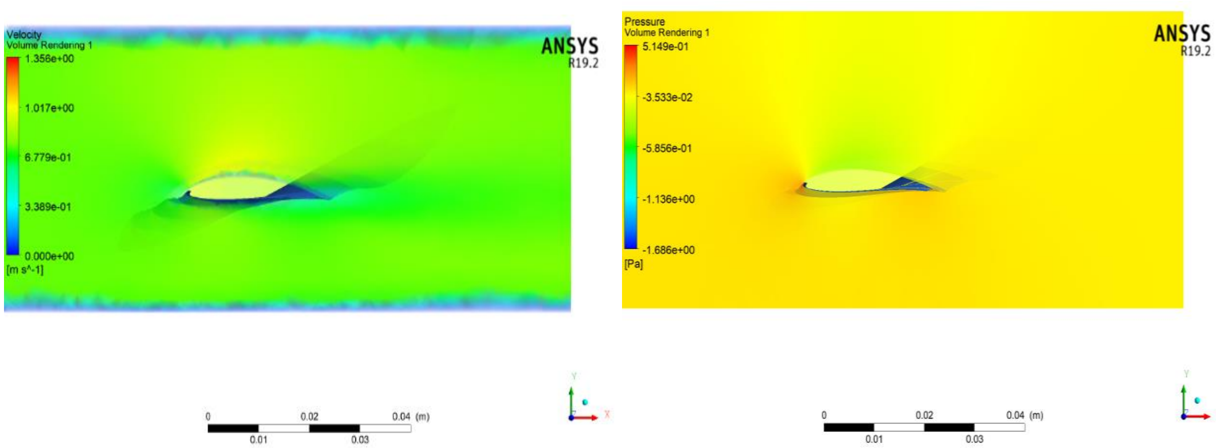

(A) (B)

Figure 5-10 (A) Velocity volume and (B) Pressure-volume

The velocity volume contour showed a flowing stream over the upper surface of the airfoil faster than the lower and the pressure contour indicate the leading edge experienced high pressure and moderate distribution on the lower surface of the airfoil.

Finally, it can see the turbulence effect on the blade during operation so the design is good, and the blade is manufactured using the design output geometry and parameters.

5.2 Experimental results and discussions

The experimental investigation to determine the AC, AC voltage, and power of the turbine. The tests were done four times in different circumstances and the velocity of water, test region of river, and rpm of the turbine are presented in table 5.1.

Table 5-1 Test criteria and dimension of river

Item	***Test1***	***Test2***	***Test3***	***Test4***
Velocity water	0.0325 m/s	>0.56m/s	0.689 m/s	0.999m/s
Area of river	7m*3m	7m*0.6m	10m*8m	10m*8m
Rpm of motor	340.723Rpm	340.723Rpm	340.723 Rpm	486.75 Rpm

The table here shows the river velocity, river area, and output rpm of the turbine, and based on this the velocity of water and rpm of motor test 1 and test 2 are conducted in the hydraulics lab, at 5-kilo campus and the result does not turn off the turbine for the test1.

It indicates there is not enough torque with the kinetic energy resulting from the indicated velocity under this test even though it cannot run the turbine alone i.e., without connecting the generator by the belt while test2 the turbine can run itself without connecting the pully with the generator.

5.2.1 Experimental results of alternating current and Voltage

Here we have discussed the rest of the test3 and test4 as well depends on the result shown below in the table 5.2.

Table 5-2 AC voltage experiment results

Times(S)	1	2	3	4	5	6	7	8	9
Voltage(V)	0.35	-1.27	1.256	-2.05	2.89	-2.76	3.14	-3.09	4.14

10	11	12	13	14	15	16	17	18	19
-3.98	2.56	-1.76	0.78	-3.08	5.27	-4.89	5.14	-4.06	4.93

20	21	22	23	24	25	26	27	28	29
-3.96	2.69	-2.89	2.79	-1.86	1.58	-2.69	2.34	-1.98	4.63

Times(S)	30	31	32	33	34	35	36	37	38	39
AC Voltage(V)	-4.05	1.09	-4.21	3.14	-2.68	2.79	-1.89	1.05	-2.09	0.79

For test 3 operated with the output rpm of 340.723 and the velocity 0.689m/s and on the same region of the river to test4.

The shown on the graph RMS value of AC voltage

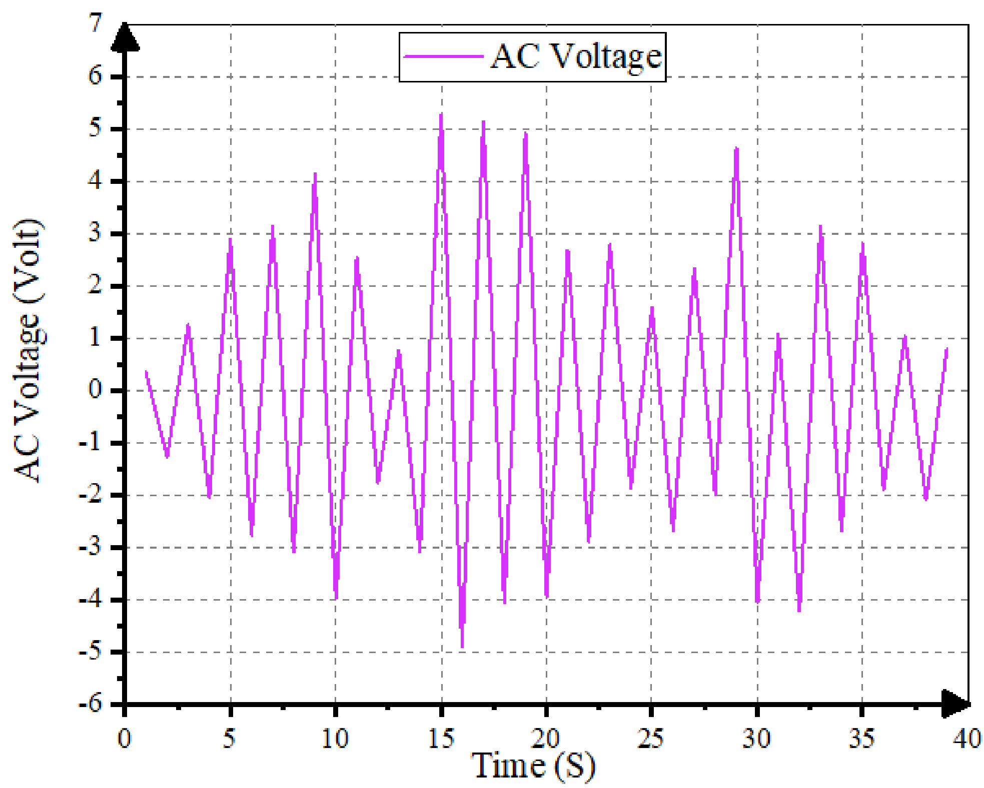

Figure 5-11 AC voltage results at velocity 0.689 m/s

But we can't get the current reading using a multimeter because as it is known that generating electricity is output rpm of the generator must be high. To generate the AC required to increase that output rpm of the generator and by doing the increasing of rpm from 340.723rpm to 486.75 rpm the last experiment was done. The test4 was done at an output rpm of 486.75 and velocity of 0.999 m/s, finally, the results are as shown below in table 5.3.

Table 5-3 Test 4 experimental AC current results at velocity of 0.999 m/s

Time(S)	1	2	3	4	5	6	7	8	9
AC current (Amp)	3.21	-3.05	1.24	-3.5	14.13	-13.52	0.48	-0.98	6.58

10	11	12	13	14	15	16	17	18	19
-5.99	2.08	-2.079	3.86	-3.98	1.8	-1.85	1.04	-1.54	2.92
20	21	22	23	24	25	26	27	28	29
-2.96	9.72	-9.87	2.23	-2.4	12.7	0.61	-4.98	5.52	-5.76

30	31	32	33	34
16.03	-15.97	6.35	-6.56	0.24

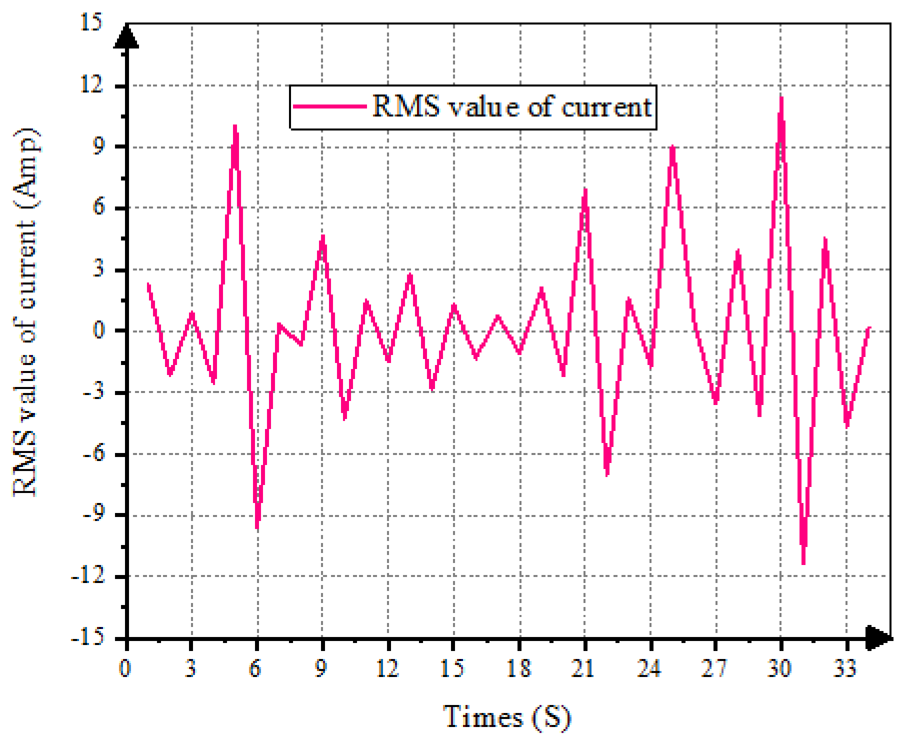

Figure 5-12 AC current curve at v=0.999m/s

As we have seen from the graph the results are is sinusoidal and imply that the experiment meets the theoretical science. However, the amplitude of AC has a variation of current with each interval of time in seconds. So, this indicates there are limitations to recording the result manually and losing mechanical components and manufacturing quality of hydrokinetic turbine. The maximum current can be extracted 16Amp and the minimum is 0.78 Amp with a radius of 130 mm radius of turbine blade and reused dc motor even with unknown motor efficiency.

The voltage coming from experimentation presented in the table below.

Table 5-4 experimental AC voltage results at velocity of 0.999m/s

Times(S)	1	2	3	4	5	6	7	8	9
AC Voltage(V)	4.28	9.48	7.46	5.79	9.47	6.58	9.23	6.54	5.96

10	11	12	13	14	15	16	17	18	19
9.11	7.45	5.76	8.77	7.62	9.35	7.89	9.69	8.46	9.498

20	21	22	23	24	25	26	27	28	29
7.55	9.49	6.58	9.32	5.82	9.58	6.31	7.89	9.51	7.79

30	31	32	33	34
4.82	8.97	9.52	9.51	8.62

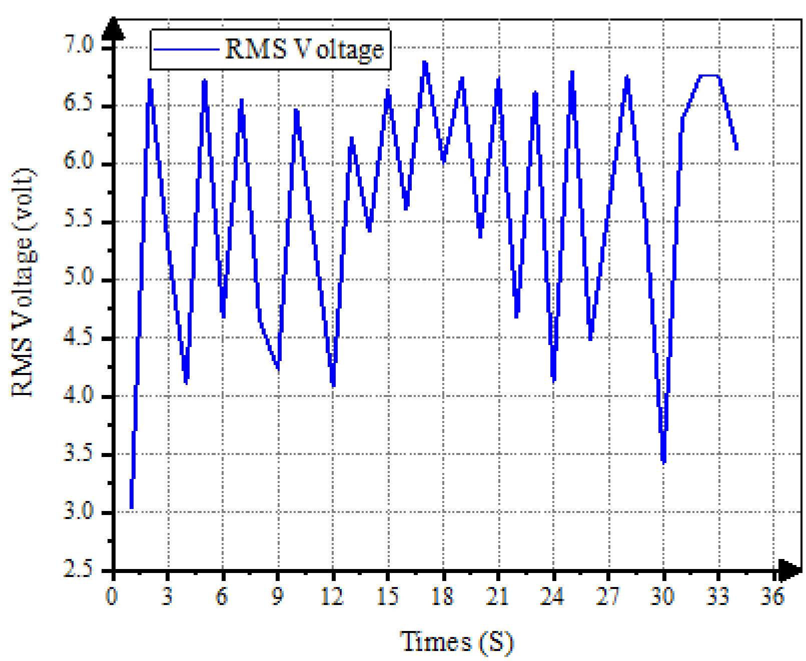

Figure 5-13 AC voltage curve at v=0.999m/s

The voltage obtained from the experiment the values are positive and its pattern is sinusoidal. In this case, the voltage reading indicates the peak-to-peak value, so all values of Ac voltage are positive. Therefore, the turbine can be producing the maximum and minimum values of voltage 9.69 and 4.28 volt respectively.

Using mathematical expression, the electrical power determines from the AC and AC voltage results coming from the experiment. As we know the power is the product of current and voltage in the circuits. So, the power found in table 5.5 below is calculated values getting from the experiment results of alternating current and AC voltage.

Table 5-5 Power coming from experiment at v=0.999m/s

Times(S)	1	2	3	4	5	6	7	8	9
Power (w)	13.7388	-28.914	9.2504	133.8111	-20.265	-88.9616	4.4304	-6.4092	39.2168

10	11	12	13	14	15	16	17	18	19	20
-54.57	15.50	-11.975	33.85	-30.33	16.83	-14.60	10.10	-13.03	27.7342	-22.35

21	22	23	24	25	26	27	28
92.2428	-64.9446	20.7836	-13.968	121.666	3.8491	-39.2922	52.4952

29	30	31	32	33	34
-44.87	77.264	-143.251	60.452	-62.39	2.0688

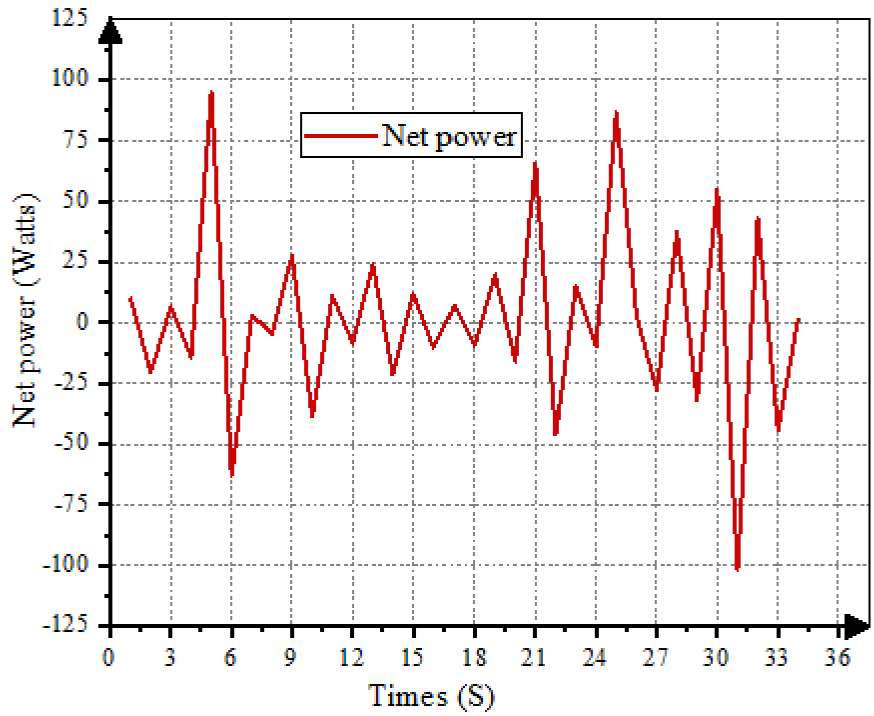

Figure 5-14 Power curves at v=0.999m/s

From the mathematical model, the power is the product of voltage and current and the relation of the graph indicates the power is more sensitive to alternating current. Because it has the same sinusoidal pattern with current but her the voltage is peak to peak value and all the values minimum to the maximum are positive.

The calculated power resulting coming from the experiment of current and voltage the minimum, maximum and, average values are 4.4304 watts, 143.251 watts and, 76 respectively and it closer to the expected outcome of the study with the diminished dimension of the blade radius 130mm with the velocity of 0.999m/s and Input and output speed of 73.012 rpm and 486.75 rpm respectively. The power curve and AC curves are having the same sinusoidal pattern may the voltage curves coming from experimentation are even different so the power was more sensitive to current when we observe the experimentation results and it obeys the theoretical science of basic electrical circuit. The graphical relationship of those power, alternating current, and voltage are shown in figure 5.15.

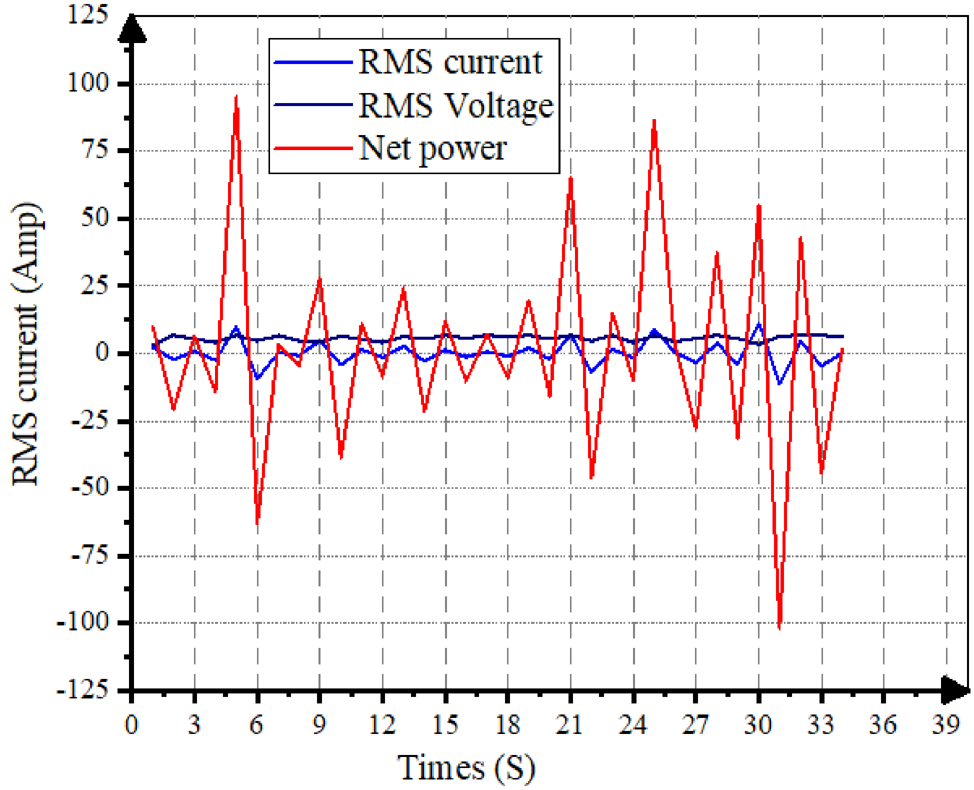

Figure 5-15 Relationship between power P, alternating current I, and AC voltage (V)

Another finding is to calculate the torque value shown in Figure 4.5 using Equation 4.36, and the result is presented in figure 5.6 as follows.

The bulb during experiment getting bulb on the last turbine set up (test 4 on table 5.1).

Figure 5-16 Lighting bulb during the experiment

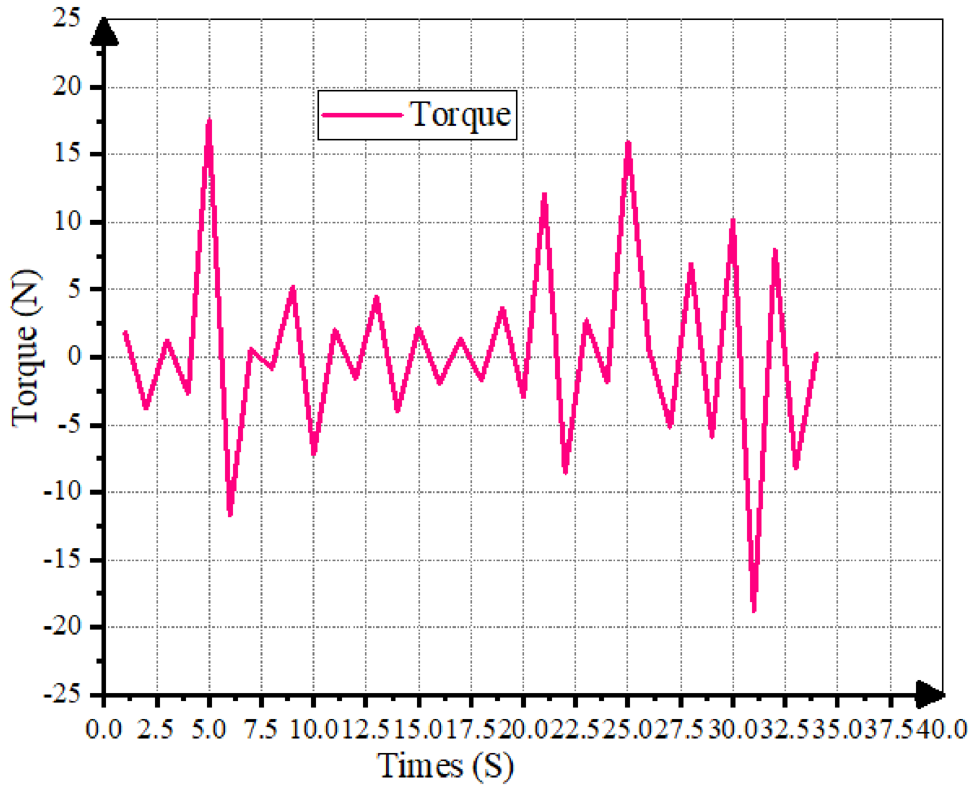

Figure 5-17 Calculated values of torque of the motor

These results are the torque with the load condition and the negative sign indicates the pole of the DC motor.

The relation of torque and power is directly proportional. The torque increases the power also increases the increasing behavior power is doubling of the torque to turn the generator during the peak-to-peak values of AC voltage. Finally, the overall efficiency of the turbine is 57.3 % and it is recommended to use the system to electrify the rural area of Ethiopia.

Table 5-6 Summary of the results

Findings	Current (Amp)	Voltage (Volt)	Power (watts)	Torque (N)
maximum	16.03	9.69	143.251	18.745
Minimum	0.78	4.28	4.43	0.3
RMS value	11.33	6.89	128.37 (net)	2.52

The results on table 4.6 get with set up of the experiment

The velocity of water is 0.999 m/s

Area of river 10m*8 m

Revolution of motor shaft 486.75 rpm

Chapter 6: Conclusions and Recommendations

6.1 Conclusions

In this study design, manufacturing, and experimental investigation of the hydrokinetic turbine was carried out geometric optimization of turbine blade and experimentation in different parameters which are velocity, size of power transmission mechanism to the desired orientation. The experiment was done at four different velocities and different output rpm of the motor delivered from the turbine. The results of the system show that the turbines displayed a viable behavior for harnessing energy in such a system. But conversion efficiencies vary as it directly depends on the velocity and velocity ratio of the transmission system. Under the same condition design parameters, an angle of attack is 5 degrees.

This is because the blade harness energy as well as accommodates and convert the onward force of tide in such condition conveniently. It can be concluded that zero head hydrokinetic turbines efficiency of conversion depends directly on the velocity, design, and manufacturing accuracy under normal flow conditions. The ability of the turbine to assimilate the water force and convert it to useful energy effectively.

The valuable results obtained experimentation are the last test with the condition of velocity 0.999m/s, radius 130mm and, output rpm of motor 486.75 and the system can generate alternating current RMS value of 11.33Amp, voltage RMS value 6.89 volts and, net power of 128.7watts and its overall efficiency of the system is 51.48%. The final result of the experiment would be used to design a suitable system for energy harvesting in rural areas especially in Ethiopia, off-grid areas where energy is insufficient and there is an abundance of flowing river water. The limitation of this work on experiment there is no digital measurements of current, voltage and power as well as its torque of motor.

6.2 Recommendations

Based on the study made above, the following recommendations are made.

- ✓ Data measuring instruments should be a proper device like an oscilloscope to avoid missing records in each second and to decrease the uncertainties in measurement.
- ✓ The manufacturing accuracy should be considered for effective energy grasping using the system
- ✓ Renewable energy technologies should be encouraged by giving incentives to make them competitive in the market.
- ✓ The government should be supported to enhance renewable energy particularly small-scale hydropower investment in the country

Future work:

In this thesis, the experiment was done only on specific airfoil S1020 by taking hydro performance analysis of angle of attack 5^0. The future work needs to do experiments with different NACA series of airfoil with different angles of attack as well as its control system when the fluctuation of flow in the river occurred.

References

[1] M. Cheever and J. Howell, "Environmental Policy Review : Key Issues in Ethiopia 2011," 2011.

[2] K. Kusakana and H. Vermaak, "Hydrokinetic power generation for rural electricity supply : Case of South Africa," no. July, 2013, doi: 10.1016/j.renene.2012.12.051.

[3] B. P. Ho-yan, "Design of a Low Head Pico Hydro Turbine for Rural Electrification in Cameroon by," 2012.

[4] S. A. E.Chica, F.perez, Arubio-Clemente, "Design of a hydrokinetic turbine," 2016, no. August, doi: 10.2495/ESUS150121.

[5] power africa, "EthiopiaCountryFactSheet__2016.09 FINAL_0," 2018.

[6] S. Karekezi, P. Balla, X. Ochieng, A. Fwd, P. O. Box, and E. M. Close, "The Potential Contribution of Non-Electrical Renewable Energy Technologies (RETs) to Poverty Reduction in East Africa By," no. December, 2005.

[7] S. Tsegaye, "Highlights of the ethiopian energy sector," 2016.

[8] A. Dalelo, "Rural Electrification in Ethiopia: opportunities and bottlenecks," *Addis Ababa Univ. Coll. Educ.*, pp. 1–13, 2003.

[9] B. Khan and P. Singh, "The current and future states of Ethiopia's energy sector and potential for green energy: A comprehensive study," *Int. J. Eng. Res. Africa*, vol. 33, no. November 2018, pp. 115–119, 2017, doi: 10.4028/www.scientific.net/JERA.33.115.

[10] M. F. Flow *et al.*, "Rural electrification projects frameworkdocuments (proto types)," 2011.

[11] T. B. Kotu, "Renewable for Rural Electrification in Ethiopia," 2010.

[12] G. E. Beyene, A. Kumie, R. Edwards, and K. Troncoso, *Opportunities for transition to clean household energy in Ethiopia Application of the WHO Household Energy Assessment Rapid Tool (HEART)*. 2018.

[13] 2019. MoWIE. National electrification program 2.0: Integrated planning for universal

access. Technical report, Ethiopian Ministry of Water, Irrigation and Electricity, "National Electrification Program 2.0," *Themat. Progr. Doc.*, no. October, p. 49, 2019,

[14] A. Afanador, M. Koper, M. Lulie, G. Tesfaye, and M. Teferra, "Off-grid Rural electrification in Ethiopia," 2016.

[15] W. Monatrakul, "The Effect of blade angleon turbine efficiency of a Spiral Horizontal Axis Hydro Turbine,2017 International Conference on Alternative Energy in Developing Countries and Emerging Economies 2017 AEDCEE, 25-26 May 2017, Bangkok, Thailand Effect," *Energy Procedia*, vol. 138, pp. 811–816, 2017, doi: 10.1016/j.egypro.2017.10.075.

[16] I. Hamzah, A. Prasetyo, D. D. D. P. Tjahjana, and S. Hadi, "Effect of blades number to performance of Savonius water turbine in water pipe," vol. 030046, no. February, pp. 1–5, 2018, doi: 10.1063/1.5024105.

[17] S. Islam, "Novel design work in energy extraction form in-srteam water by various types of micro hydroturbines," *researchgate*, no. January, 2017.

[18] T. Putranto and A. Sulisetyono, "Lift-Drag Coefficient and Form Factor Analyses of Hydrofoil due to The Shape and Angle of Attack," vol. 12, no. 21, pp. 11152–11156, 2017.

[19] J. Aguilar, A. Rubio-clemente, and L. Velasquez, "Design and Optimization of a Multi-Element Hydrofoil for a Horizontal-Axis Hydrokinetic Turbine," 2019.

[20] Y. Yining, "Analysis of the Influence of Camber on Hydrodynamic Characteristics of Airfoil Based on FLUENT," 2020, doi: 10.1088/1742-6596/1519/1/012020.

[21] and H. B. M. Nachtane1, M. Tarfaoui, A. El Moumen, D. Saifaoui, "Design and Hydrodynamic Performance of a Horizontal Axis Hydrokinetic Turbine," *Int. J. Automot. Mech. Eng.*, vol. 16, no. 2, pp. 6453–6469, 2019, doi: 10.15282/ijame.16.2.2019.1.0488.

[22] K. A. R. Ismail[1] and T. P. Batalha, "A comparative study on river hydrokinetic turbines blade profiles," *J. Eng. Res. Appl. www.ijera.com ISSN*, vol. 5, no. 51, pp. 2248–962201, 2015, [Online]. Available: www.ijera.com.

[23] M. S. Guney, "Evaluation and measures to increase performance coefficient of hydrokinetic

turbines," *Renew. Sustain. Energy Rev.*, vol. 15, no. 8, pp. 3669–3675, 2011, doi: 10.1016/j.rser.2011.07.009.

[24] A. Rachman, R. Balaka, J. Delly, and Y. Gunawan, "Simulation on the effect of the blade number on the rotational characteristic on a horizontal axis river current turbine," 2013.

[25] P. A. S. F. Da Silva, L. D. Shinomiya, T. F. De Oliveira, J. R. P. Vaz, A. L. A. Mesquita, and A. C. P. B. Junior, "Design of Hydrokinetic Turbine Blades Considering Cavitation," *Energy Procedia*, vol. 75, pp. 277–282, 2015, doi: 10.1016/j.egypro.2015.07.343.

[26] A. Muratoglu and M. I. Yuce, "Performance Analysis of Hydrokinetic Turbine Blade Sections," no. January 2016, 2015.

[27] S. A. Oller and L. Nallim, "The usability of the Selig S1223 profile airfoil as a high lift hydrofoil for hydrokinetic application," vol. 9, no. 3, 2016.

[28] P. Augusto *et al.*, "Analysis of cavitation for the optimized design of hydrokinetic turbines using BEM," *Appl. Energy*, vol. 185, pp. 1281–1291, 2017, doi: 10.1016/j.apenergy.2016.02.098.

[29] S. A. O. Aramayo, L. G. Nallim, and S. Oller, *A river bed hydrokinetic turbine . A laminated composite material rotor design A river bed hydrokinetic turbine .*, no. February. 2017.

[30] P. Adhikary, P. K. Roy, A. Mazumdar, A. Mechanical, and S. V. I. S. T. Wbut, "Selection of Hydro-Turbine Blade Material : Application of Fuzzy Logic (MCDA)," vol. 3, no. 1, pp. 426–430, 2013.

[31] C. L. Rantererung, S. Soeparman, R. Soenoko, and S. Wahyudi, "The dual nozzle cross flow turbine performance," *ARPN J. Eng. Appl. Sci.*, vol. 11, no. 13, pp. 8538–8543, 2016.

[32] K. W. Tan, B. Kirke, and M. Anyi, "Small-scale hydrokinetic turbines for remote community electrification," *Energy Sustain. Dev.*, vol. 63, pp. 41–50, 2021, doi: 10.1016/j.esd.2021.05.005.

[33] P. M. M. Das and R. S. Amano, "Basic Theory for Wind Turbine Blade Aerodynamics," in *Airodynamics of wind turbine*, vol. 81, us: WIT Press, 2014.

[34] J. Ledoux *et al.*, “Analysis of the Blade Element Momentum Theory To cite this version : HAL Id : hal-02550763,” 2020.

[35] Taylor & Francis Group, Ed., *wind turbine technology A.R. Jha.ph.d.,* 2011th ed. Printed in the United States of America on acid-free paper 10 9 8 7 6 5 4 3 2 1.

[36] W. Q. Wang, R. Yin, and Y. Yan, “Design and prediction hydrodynamic performance of horizontal axis micro-hydrokinetic river turbine,” *Renew. Energy*, vol. 133, pp. 91–102, 2019, doi: 10.1016/j.renene.2018.09.106.

[37] B. Principles, “George E. Heckes, PE, Allen, PE Alden Research labratory How to Evaluate Hydrokinetic Turbine Performance and Loads,” *white Pap.*

[38] J. Sarja and V. Halonen, “Wind turbine selection criteria: a customer perspective,” *Artic. J. Power Energy Eng.*, vol. 7, no. September 2013, pp. 1795–1802, 2013, [Online]. Available: https://www.researchgate.net/publication/271191500.

[39] Z. Hu and X. Du, “Reliability analysis for hydrokinetic turbine blades,” *Renew. Energy*, vol. 48, pp. 251–262, 2012, doi: 10.1016/j.renene.2012.05.002.

[40] Hydro-Québec, “Renewable Energy Option Hydrokinetic Power,” *Bibliothèque Arch. Natl. du Québec*, p. 9, 2015, [Online]. Available: http://www.hydroquebec.com/sustainable-development/documentation-center/hydrokinetic-power.html.

[41] C. A. Bustamante, W. F. Florez, H. Power, and A. F. Hill, “Hydrokinetic turbine location analysis by a local collocation method with Radial Basis Functions for two-dimensional Shallow Water equations,” *WIT Trans. Ecol. Environ.*, vol. 195, no. September, pp. 3–13, 2015, doi: 10.2495/ESUS150011.

[42] G. Getenet and Y. Damtew, “Technical and Socio Economic Assessment of Water Mill Sites for Micro Hydro Power Generation in North Shoa Zone of Amhara Region,” vol. 7, no. 2, pp. 45–48, 2019, doi: 10.11648/j.ajee.20190702.11.

[43] J. G. M. A. L. R. J.F. Manwell, *wind energy explained theory, design and application*. New York: John Wiley & Sons Ltd Baffins Lane, Chichester, West Sussex PO19 IUD, England, 2002.

[44] G. Energy, *Green Energy Technology, Introduction to wind energy systems basics, Technology and operation*, Springer S. London New York Springer: springer.

[45] M. Anyi and B. Kirke, “Energy for Sustainable Development Hydrokinetic turbine blades : Design and local construction techniques for remote communities,” *Energy Sustain. Dev.*, vol. 15, no. 3, pp. 223–230, 2011, doi: 10.1016/j.esd.2011.06.003.

[46] “Airfoil lift and drag polar diagrams.” http://airfoiltools.com/polar/index (accessed Jul. 27, 2021).

[47] “www.inmtn.com.” https://www.inmtn.com/tools/float-method/.

[48] Q. Studies, M. Programmes, and R. Ballance, “Chapter 12 - hydrological measurments,” 1996.

[49] W. Tian, Z. Mao, and H. Ding, “Design , test and numerical simulation of a low-speed horizontal axis hydrokinetic turbine,” *Int. J. Nav. Archit. Ocean Eng.*, vol. 10, no. 6, pp. 782–793, 2018, doi: 10.1016/j.ijnaoe.2017.10.006.

[50] and M. B. Robert Thresher, Al LiVecchi, Ye Li, Scott Hughes, Jason Jonkman, David Maniaci, “HARP_Opt: Horizontal Axis Rotor Performance Optimization | Wind Research | NREL.” https://www.nrel.gov/wind/nwtc/harp-opt.html (accessed Jul. 21, 2021).

[51] S. Mathew, *Sathyajith Mathew Wind Energy Fundamentals, Resource Analysis and Economics*. .

[52] C. Lancashire, P. Sciences, and C. Lancashire, “Aerodynamics Analysis of Small Horizontal Axis Wind Turbine Blades by Using 2D and 3D CFD Modelling Engineering and Physical Sciences at the University of Central Lancashire ,” 2011.

[53] W. C. Schleicher and R. C. Klein, “Numerical Optimization of a Portable Hydrokinetic Turbine,” no. June, 2014.

[54] L. K. Gaur, M. K. Gaur, and P. C. S. Malvi, “Cfd analysis on wind blade,” no. August, 2018.

[55] R.S. KHURMI J.K. GUPTA, *A textbook of Machine Design*, 14 edditio., no. I. EURASIA PUBLISHING HOUSE (PVT.) LTD, 2005.

[56] J. A. Sainz, “New Wind Turbine Manufacturing Techniques,” *Procedia Eng.*, vol. 132, pp. 880–886, 2015, doi: 10.1016/j.proeng.2015.12.573.

[57] N. Shahrubudin, T. C. Lee, and R. Ramlan, “An overview on 3D printing technology: Technological, materials, and applications,” *Procedia Manuf.*, vol. 35, no. August, pp. 1286–1296, 2019, doi: 10.1016/j.promfg.2019.06.089.

[58] S. C. Joshi and A. A. Sheikh, “3D printing in aerospace and its long-term sustainability,” *Virtual Phys. Prototyp.*, vol. 10, no. 4, pp. 175–185, 2015, doi: 10.1080/17452759.2015.1111519.

[59] R. V. Aroca, C. E. H. Ventura, I. De Mello, and T. F. P. A. T. Pazelli, “Sequential additive manufacturing: Automatic manipulation of 3D printed parts,” *Rapid Prototyp. J.*, vol. 23, no. 4, pp. 653–659, 2017, doi: 10.1108/RPJ-02-2016-0029.

[60] A. Uriondo, M. Esperon-Miguez, and S. Perinpanayagam, “The present and future of additive manufacturing in the aerospace sector: A review of important aspects,” *Proc. Inst. Mech. Eng. Part G J. Aerosp. Eng.*, vol. 229, no. 11, pp. 2132–2147, 2015, doi: 10.1177/0954410014568797.

[61] A. Ramya and S. L. Vanapalli, “3D printing technologies in various applications,” *Int. J. Mech. Eng. Technol.*, vol. 7, no. 3, pp. 396–409, 2016.

[62] S. Farah, D. G. Anderson, and R. Langer, “Physical and mechanical properties of PLA, and their functions in widespread applications — A comprehensive review,” *Adv. Drug Deliv. Rev.*, vol. 107, pp. 367–392, 2016, doi: 10.1016/j.addr.2016.06.012.

[63] M. Jamshidian, E. A. Tehrany, M. Imran, and M. Jacquot, “Poly-Lactic Acid : Production , Applications , Nanocomposites , and Release Studies,” vol. 9, pp. 552–571, 2010, doi: 10.1111/j.1541-4337.2010.00126.x.

[64] L. U. Stephen Helba, Emeritus, Ed., *Electrical Machines Drives and Power System.pdf*, Fith editi. New Jersey Columbus, Ohio: Charles E. Stewart, Jr.

[65] E. Engineering, “ELL 100 - Introduction to Electrical Engineering L LECTURE 13: SINGLE PHASE AC CIRCUITS,” .

Appendix

Figure 1 Overall assembly of hydrokinetic turbine

Figure 2 Turbine and bulb during the experiment

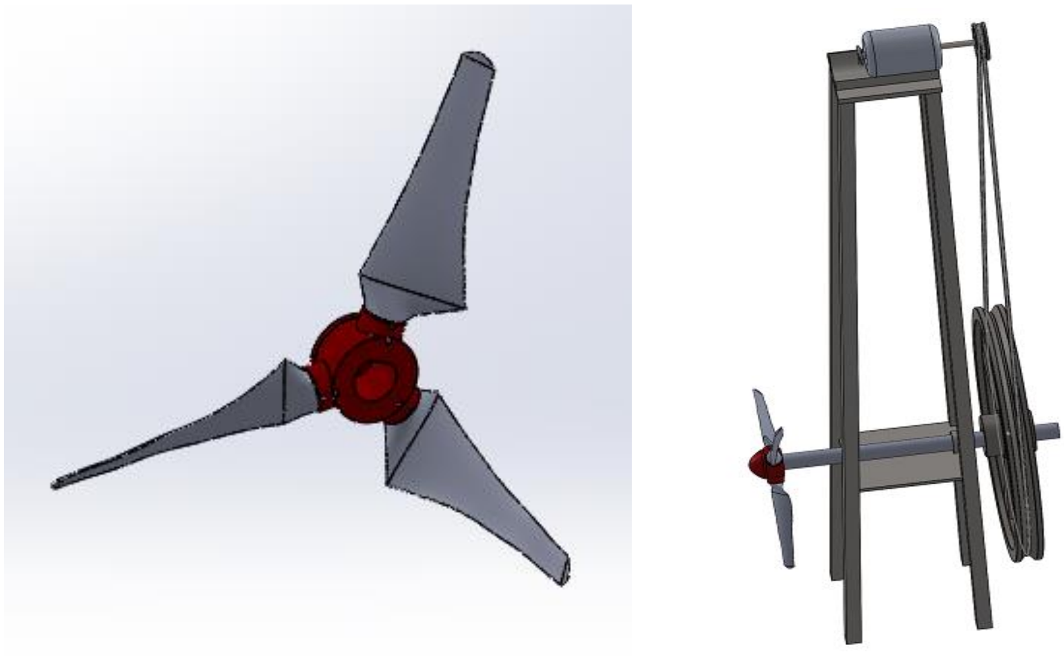

Figure 3 Overall 3D model assembly of turbine and blade

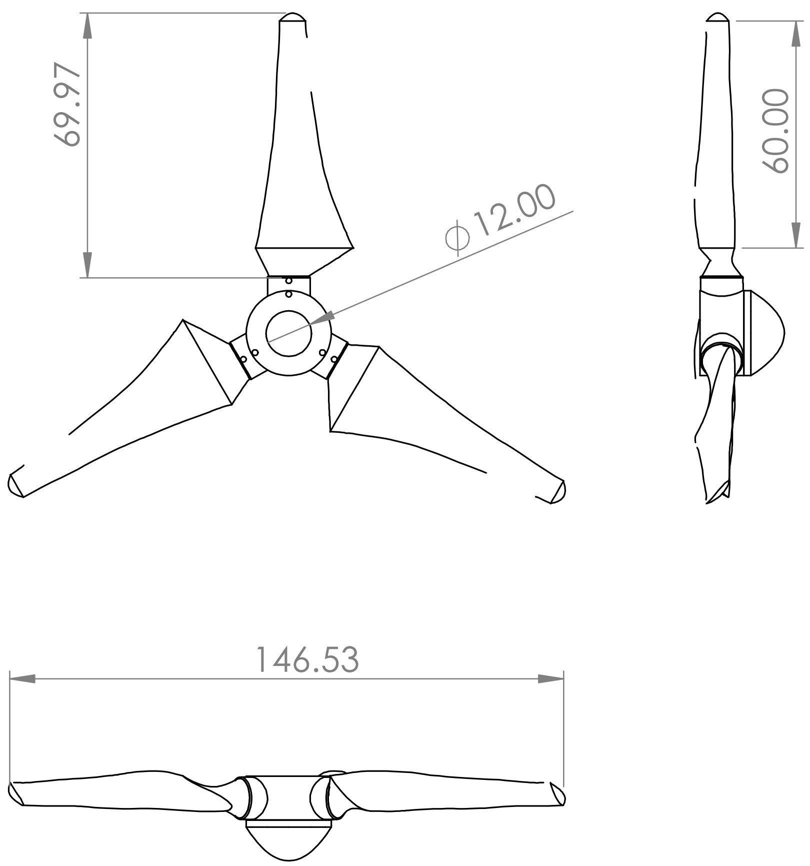

UNLESS OTHERWISE SPECIFIED: DIMENSIONS ARE IN MILLIMETERS SURFACE FINISH: TOLERANCES: LINEAR: ANGULAR:	FINISH:	DEBURR AND BREAK SHARP EDGES	DO NOT SCALE DRAWING / REVISION

	NAME	SIGNATURE	DATE
DRAWN	Teklemariam Tadesse		
CHK'D	Dr. Abdulkadir A.		
APPV'D	Dr. Abdulkadir A.		
MFG			
Q.A			

TITLE: Blade and hub assembly

MATERIAL: PLA(polylactic acid)

DWG NO. 1

WEIGHT:

SCALE:1:2

SHEET 1 OF 1

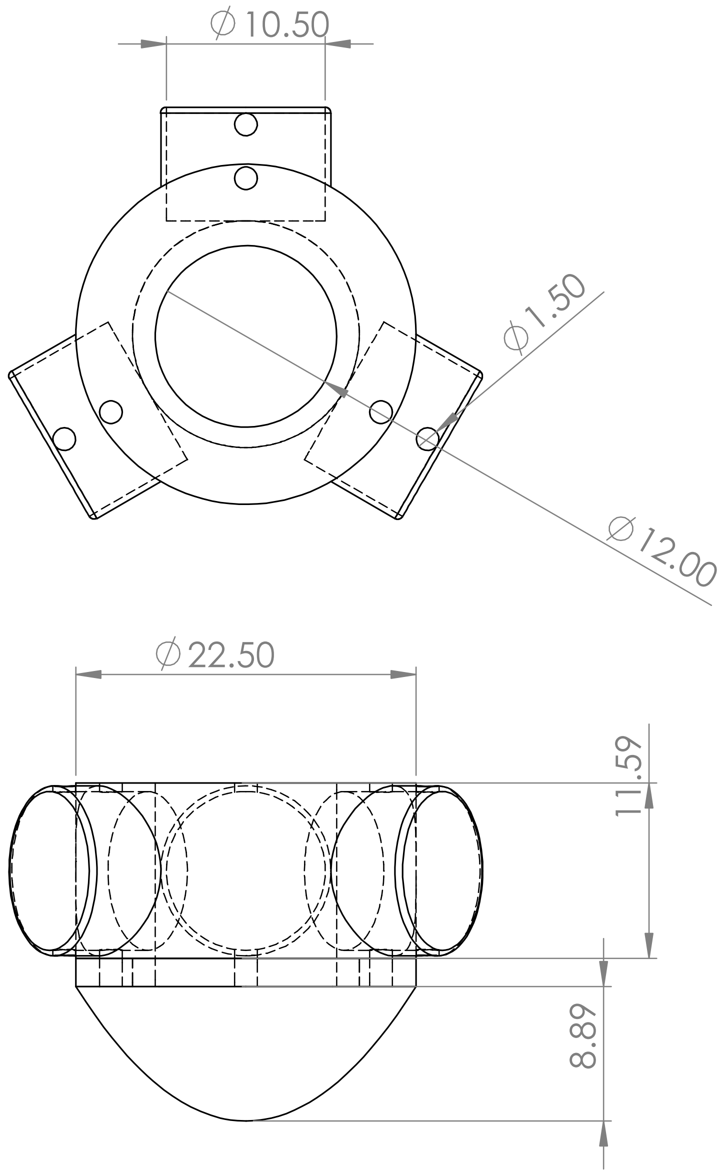

UNLESS OTHERWISE SPECIFIED:
DIMENSIONS ARE IN MILLIMETERS
SURFACE FINISH:
TOLERANCES:
LINEAR:
ANGULAR:

FINISH:

DEBURR AND BREAK SHARP EDGES

DO NOT SCALE DRAWING

REVISION

	NAME	SIGNATURE	DATE
DRAWN	Teklemariam Tadesse		
CHK'D	Dr. Abdulkadir A.		
APPV'D	Dr. Abdulkadir A.		
MFG			
Q.A			

TITLE: .hub and cup

MATERIAL: PLA (Polylactic Acid

DWG NO 2

A4

WEIGHT:

SCALE:1:2

SHEET 1 OF 1

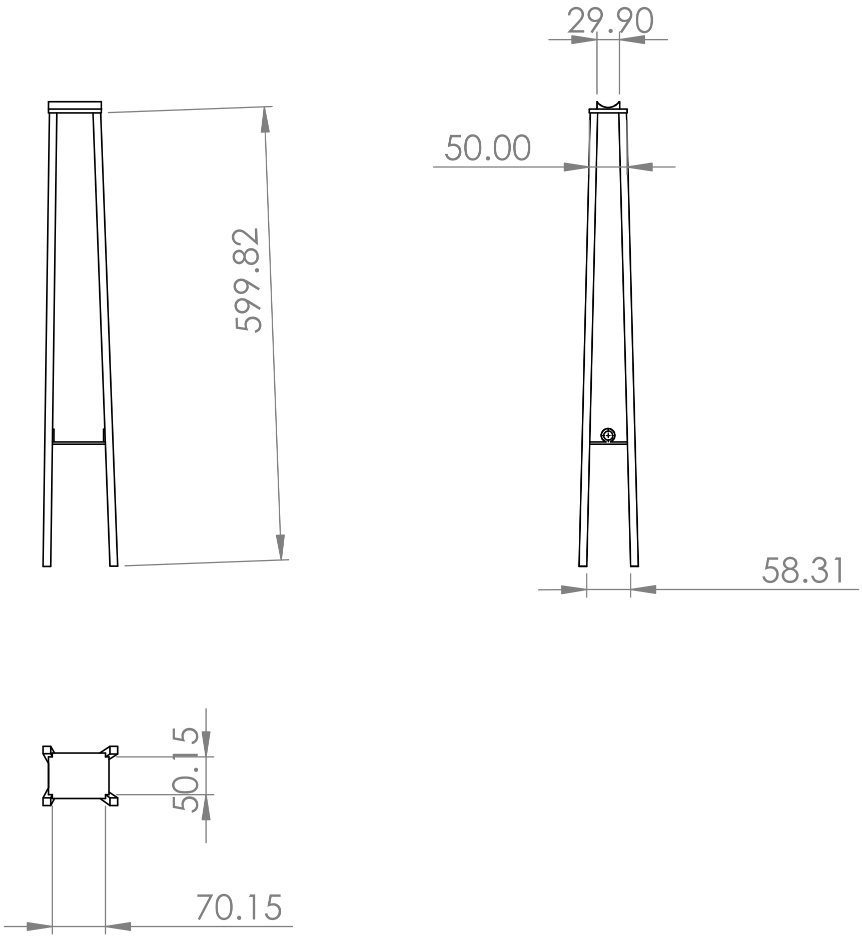

UNLESS OTHERWISE SPECIFIED:
DIMENSIONS ARE IN MILLIMETERS
SURFACE FINISH:
TOLERANCES:
LINEAR:
ANGULAR:

FINISH:

DEBURR AND BREAK SHARP EDGES

DO NOT SCALE DRAWING

REVISION

	NAME	SIGNATURE	DATE
DRAWN	Teklemariam Tadesse		
CHK'D	Dr. Abdulkadir A.		
APPV'D	Dr. Abdulkadir A.		
MFG			
Q.A			

TITLE: Stand

MATERIAL: RHS metal

DWG NO. 3

A4

WEIGHT:

SCALE:1:1

SHEET 1 OF 1

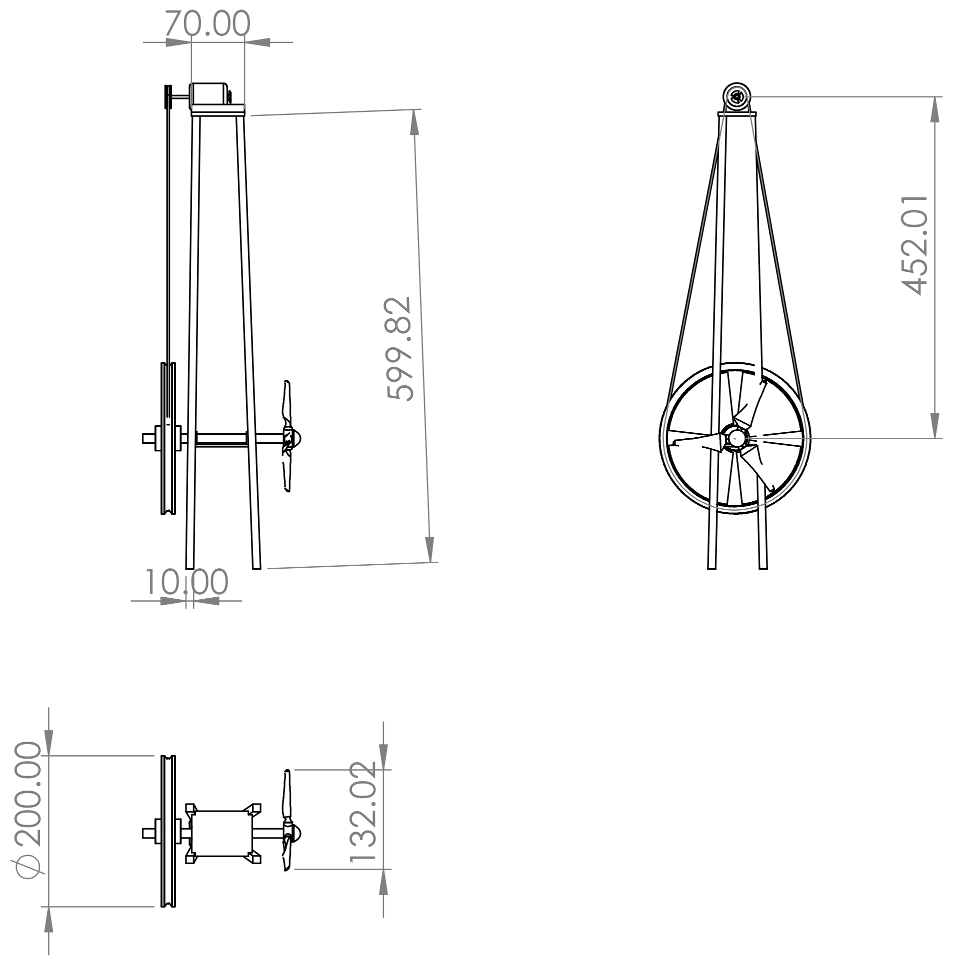

UNLESS OTHERWISE SPECIFIED:
DIMENSIONS ARE IN MILLIMETERS
SURFACE FINISH:
TOLERANCES:
LINEAR:
ANGULAR:

FINISH:

DEBURR AND BREAK SHARP EDGES

DO NOT SCALE DRAWING

REVISION

	NAME	SIGNATURE	DATE
DRAWN	Teklemariam Tadesse		
CHK'D	Dr. Abdulkadir A.		
APPV'D	Dr. Abdulkadir A.		
MFG			
Q.A			

TITLE: full Assembly of turbine

MATERIAL: RHS metal and PLA

DWG NO. 4

WEIGHT:

SCALE:1:1

SHEET 1 OF 1

Table 0-1 Turbine blade design data

se.No	r(m)	alpha	CpD	lampda r	1/LAMPDA	phi	BETA	1-COS PHI	(8*PI*r)/(3*CLD)		chord(m)	chord/3	R(m)
1	0.1374	5	1.1643	1.4	0.714285714	23.69178519	18.69178519	0.084279787	0.988143949		0.083280561	0.027760187	0.687
2	0.19983	5	1.1643	2.03611354	0.491131748	17.43808017	12.43808017	0.045958632	1.437123765		0.066048242	0.022016081	
3	0.26226	5	1.1643	2.67222707	0.374219695	13.67789263	8.677892626	0.028359569	1.886103582		0.053489085	0.017829695	
4	0.32469	5	1.1643	3.30834061	0.302266338	11.21219979	6.212199792	0.019086225	2.335083398		0.044567926	0.014855975	
5	0.38712	5	1.1643	3.94445415	0.253520503	9.483953547	4.483953547	0.013668213	2.784063214		0.03805317	0.01268439	
6	0.44955	5	1.1643	4.58056769	0.218313552	8.210146946	3.210146946	0.010249044	3.23304303		0.0331356	0.0110452	
7	0.51198	5	1.1643	5.21668122	0.191692756	7.234364304	2.234364304	0.007960648	3.682022846		0.029311289	0.00977043	
8	0.57441	5	1.1643	5.85279476	0.170858546	6.46389858	1.46389858	0.006357013	4.131002663		0.02626084	0.008753613	
9	0.63684	5	1.1643	6.4889083	0.154109128	5.840587079	0.840587079	0.005191127	4.579982479		0.02377527	0.00792509	
10	0.69927	5	1.1643	7.12502183	0.140350447	5.326201733	0.326201733	0.004317648	5.028962295		0.021713287	0.007237762	
11	0.7617	5	1.1643	7.76113537	0.128847128	4.894630423	-0.105369577	0.003646703	5.477942111		0.019976429	0.00665881	